AGU PUBLICATIONS

JGR

Journal of Geophysical Research: Atmospheres

RESEARCH ARTICLE
10.1002/2013JD020316

Key Points:
- A monthly mean global sea ice concentration data set from 1850 is constructed
- Passive microwave data are combined with historical sources
- Adjustments are calculated using periods of data overlaps to achieve homogeneity

Correspondence to:
H. A. Titchner,
holly.titchner@metoffice.gov.uk

Citation:
Titchner, H. A., and N. A. Rayner (2014), The Met Office Hadley Centre sea ice and sea surface temperature data set, version 2: 1. Sea ice concentrations, *J. Geophys. Res. Atmos.*, *119*, 2864–2889, doi:10.1002/2013JD020316.

Received 7 JUN 2013
Accepted 30 DEC 2013
Accepted article online 4 JAN 2014
Published online 19 MAR 2014

The Met Office Hadley Centre sea ice and sea surface temperature data set, version 2: 1. Sea ice concentrations

Holly A. Titchner[1] **and Nick A. Rayner**[1]

[1]Met Office Hadley Centre, Exeter, UK

Abstract We present a new version of the sea ice concentration component of the Met Office Hadley Centre sea ice and sea surface temperature data set, HadISST.2.1.0.0. Passive microwave data are combined with historical sources, such as sea ice charts, to create global analyses on a 1° grid from 1850 to 2007. Climatology was used when no information about the sea ice was available. Our main aim was to create a homogenous data set by calculating and applying bias adjustments using periods of overlaps between the different data sources used. National Ice Center charts from 1995 to 2007 have been used as a reference to achieve this. In particular, large bias adjustments have been applied to the passive microwave data in both the Antarctic and Arctic summers. Overall, HadISST.2.1.0.0 contains more ice than HadISST1.1, with higher concentrations, shorter marginal ice zones, and larger extents and areas in some regions and periods. A new method for estimating the concentrations within the ice pack using the distance from the ice edge has been developed and evaluated. This was used when only the extents were known or the original concentration fields were heterogeneous. A number of discontinuities in the HadISST1.1 record are no longer found in HadISST.2.1.0.0.

1. Introduction

This paper is the first of a three-part series describing the development of version 2.1.0.0 of the Met Office Hadley Centre sea ice and sea surface temperature data set, HadISST.2.1.0.0. It contains global fields of monthly sea surface temperature (SST) and sea ice concentrations on a regular 1° longitude by 1° latitude grid, from 1850 to 2007 (see section 5 for information on further updates). This first part describes the development of the sea ice concentrations, whereas the second paper, currently in preparation by Kennedy et al., focuses on the SST component. The final part, currently in preparation by Rayner et al., describes the combination of the two analyses as well as further products, such as the estimation of a daily 0.25° resolution product from the monthly 1° analyses.

The HadISST sea ice data set is used by climate researchers for a number of different purposes. For example, it is used for the evaluation of coupled atmosphere-ocean climate models [e.g., *Keen et al.*, 2013; *Hewitt et al.*, 2011; *The HadGEM2 Development Team*, 2011; *McLaren et al.*, 2006], for the forcing of atmospheric models and dynamical reanalyses in the reproduction of recent climate [*Scaife et al.*, 2009; *Kusunoki et al.*, 2009; *Uppala et al.*, 2005; *Compo et al.*, 2011], and in the assessment of model projections [*Stroeve et al.*, 2007, 2012]. Regular monthly updates also make it an option for climate monitoring, for example, in the monitoring of the summer Arctic sea ice, which is known to be declining at a rapid rate [*Meier et al.*, 2007; *Stroeve et al.*, 2011; *Cavalieri and Parkinson*, 2012]. Sea ice concentrations can also be used to estimate SST in nearby areas of water [*Rayner et al.*, 2003]. To fulfil some of the user requirements, HadISST is a globally complete product, which inevitably means that information in some grid boxes has been estimated. In cases where whole regions or periods are missing, the sea ice is based on climatology. Care must therefore be taken when using the data set for climate monitoring, variability, or trend studies.

The aim of this work is to improve upon HadISST1.1 [*Rayner et al.*, 2003], primarily by using new data sources that have become available and by applying bias adjustments. There is also a known discrepancy in the time series of HadISST1.1 Arctic sea ice in 1996/1997 [*Stroeve et al.*, 2007; *Meier et al.*, 2007, 2012] due to a change in the source of passive microwave retrievals. A switch of passive microwave sensor at the start of 2009 resulted in a discontinuity in both the Arctic and Antarctic concentrations then. HadISST1.1 contains limited bias adjustments due to a lack of overlaps between different data sources that were available at the time of

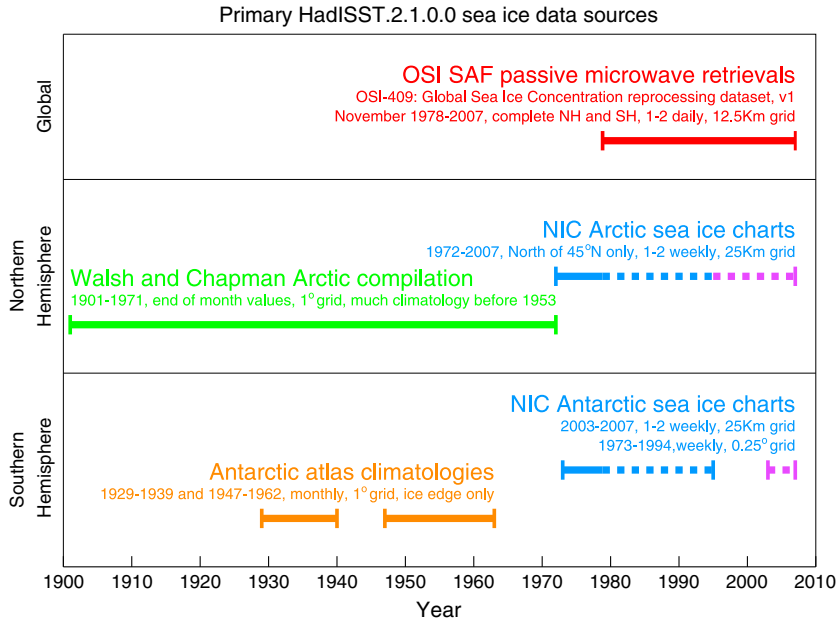

Figure 1. A timeline outlining the primary sources of sea ice data used in HadISST.2.1.0.0, including information about the product grids and resolution. Dashed lines indicate data used for the calculation of bias adjustments only. Purple dashed lines indicate the post-1994 NIC ice chart data that were used as a reference in the bias adjustment calculations.

the data set construction. Other discontinuities are therefore likely to exist, for example, at the start of the passive microwave record in 1979 [*Notz and Marotzke*, 2012]. *Meier et al*. [2012] have also attempted to produce a more consistent time series from 1953 to 2011, although only for sea ice extents in the Arctic. We aim here to make a more consistent global record of sea ice concentrations than provided in HadISST1.1 by using new data sources, applying new bias adjustments, and improving the method used in the estimation of concentrations when only information about the ice edge is known. Through using bias adjustments developed from overlap periods between data sources, we also aim for an internally consistent record.

Section 2 of this paper describes the data sources used, beginning with passive microwave retrievals and then focusing on the earlier historical sources. In section 3 we describe the HadISST.2.1.0.0 data set construction in detail, including the processing of each individual source, any bias adjustments, and the estimation of concentrations when only information on the position of the ice edge is known. Section 4 presents the resulting data set and compares it with other sea ice products. Conclusions and discussion are given in section 5, which also includes suggestions of future work and information about forthcoming data set updates and availability.

2. Data Sources

It is necessary to use a number of data sources to create a long-term time series of sea ice concentrations that extends back prior to the satellite era. The spatial and temporal coverage for each of the sources used within this analysis is summarized in Figure 1. In this section we describe the sources used and highlight the pros and cons of the different types of data.

2.1. Ocean and Sea Ice Satellite Application Facility Passive Microwave Retrievals

Passive microwave sensors have provided a continuous source of information about sea ice since October 1978, when the Scanning Multichannel Microwave Radiometer (SMMR) instrument on board NASA's Nimbus 7 satellite provided passive microwave retrievals every other day until August 1987. From July 1987, the Special Sensor Microwave/Imager (SSM/I) and Special Sensor Microwave Imager/Sounder (SSMI/S) sensors on board the Defense Meteorological Satellite Program (DMSP) series of satellites have monitored the sea ice daily and continue to do so.

Passive microwave sea ice observations from the Electrically Scanning Microwave Radiometer (ESMR) aboard NOAA's Nimbus 5 satellite are available from December 1972 to December 1976. However, unlike the more recent SMMR, SSM/I, and SSMI/S sensors, which have provided multichannel measurements, the ESMR sensor only provided single-channel measurements. It is therefore necessary to process the ESMR brightness temperatures using a different (single-channel) algorithm [*Parkinson et al*., 2004] (http://nsidc.org/data/nsidc-0009.html). Not only is there a gap in the passive microwave time series from January 1977 to September 1978 (when ESMR data are combined with the later data), but there is a lack of an overlap period with the SMMR sensor to ensure consistency. Unlike *Meier et al*. [2012], we therefore chose not to use the ESMR data within this study.

A number of algorithms have been developed to estimate sea ice concentrations from the brightness temperatures recorded by the passive microwave multichannel sensors, starting with the NASA Team algorithm [*Cavalieri et al*., 1984] and the Bootstrap algorithm [*Comiso*, 1986]. Since then a number of other algorithms have been developed. More recently, passive microwave sea ice concentration retrievals have been reprocessed by the European Organisation for the Exploitation of Meteorological Satellites (EUMETSAT) Ocean and Sea Ice Satellite Application Facility (OSI SAF) back to October 1978 using a hybrid algorithm [*European Organisation for the Exploitation of Meteorological Satellites* (*EUMETSAT*) *Ocean and Sea Ice Satellite Application Facility*, 2010] (http://osisaf.met.no/p/ice/#conc-reproc). This hybrid algorithm is a combination of the Bootstrap algorithm in frequency mode [*Comiso*, 1986] and the Bristol algorithm [*Smith*, 1996; *Hanna and Bamber*, 2001]. These algorithms have been chosen to reduce sources of error. *Andersen et al*. [2006] found that the Bootstrap algorithm in frequency mode had the lowest sensitivity to atmospheric noise over open water, and *Andersen et al*. [2007] found that the Bristol algorithm had low sensitivity to atmospheric emission, particularly at high concentrations. OSI SAF therefore gave high weighting to the Bootstrap frequency mode algorithm at low concentrations and high weighting to the Bristol algorithm at high concentrations. It is the first passive microwave sea ice concentration product to include uncertainty estimates for each retrieved value (these are given as a standard deviation). Data are available on a 12.5 km EASE (Equal-Area Scalable Earth) grid (as well as a polar stereographic grid).

Sea ice concentrations based on passive microwave retrievals have a number of known limitations, especially due to the impact of surface conditions. These include the underestimation of ice due to the presence of melt ponds on the surface of the ice in the Arctic during summer [*Inoue et al*., 2008; *Andersen et al*., 2007] and snow and slush (a mixture of snow and grease ice) [*Shokr and Kaleschke*, 2012; *Andersen et al*., 2007]. New/thin ice is also notoriously hard to detect from passive microwave retrievals [*Shokr and Kaleschke*, 2012; *The Joint WMO-IOC Technical Commission for Oceanography and Marine Meteorology*, 2008]. Other problems include land contamination around the coasts and weather effects (due to wind roughening over open water or water vapor in the atmosphere) [*EUMETSAT Ocean and Sea Ice Satellite Application Facility*, 2010; *Andersen et al*., 2007]. These effects are not fully accounted for in the OSI SAF uncertainty estimates. Despite these problems, passive microwave data provide a consistent record of concentrations, with a high temporal and spatial resolution and near-complete coverage. This provides many advantages over using any alternatives (such as sea ice charts; see section 2.2).

In this paper we use version 1.0 of the OSI SAF reprocessed passive microwave sea ice concentrations, which covers the period 25 October 1978 to 31 December 2007. The latest version of the OSI SAF product (v1.1) has been updated to 24 October 2009 with uncertainties, and a new product is planned for 2014 that will provide a subsequent update as well as further regular daily updates with a 16 day lag (S. Eastwood, OSI SAF, personal communication, 2013). It is for these reasons (as well as the hybrid algorithm used) that we chose the OSI SAF passive microwave product as the primary data source for HadISST.2.1.0.0.

2.2. Sea Ice Charts

There are a number of different ice services around the world that operationally produce sea ice charts for navigational purposes. These charts are compiled by ice analysts, who visually interpret the variety of sources of sea ice information that are available to them. Polygons are drawn on each chart, which depict areas of ice that show particular characteristics and are of a given concentration (or concentration range). The analysts utilize their expert knowledge to decide which sources to base their analysis on in different situations (e.g., when melt ponds are present, when weather contamination is seen, or when particular types of ice are present).

Early sea ice charts, produced prior to the satellite era, were manually drawn on paper and based on observations from polar meteorological stations, ships, and air reconnaissance. The lack of high-quality data meant that the charts often contained less detail than current charts. As the number of data sources increased over the last few decades, charts were based on retrievals from passive and then active satellite instruments. The many changes in the quantity and resolution of the data sources, and improvements in analysis techniques, have resulted in inhomogeneous records of sea ice concentrations from charts and increases of chart detail through time. Charts have become increasingly accurate, particularly since the mid-1990s when high-resolution synthetic aperture radar (SAR) C-band data from the RADARSAT-1 satellite became available and were preferentially used to inform charts [*The Joint WMO-IOC Technical Commission for Oceanography and Marine Meteorology*, 2008]. SAR is an active microwave instrument that produces high-resolution imagery (with a nominal resolution of 8–100 m depending on the mode) of the Earth's surface in all weather conditions. Sea ice typically reflects more radar waves than open water, making the two easy to distinguish from the images. However, the results are dependent on the physical properties of the ice (such as the type of ice), making the images useful for the production of detailed operational ice charts but complex to interpret. SAR data are available at a cost, and the coverage each day is dependent on location and spatial resolution of the beam modes used (see the Canadian Space Agency website for more information, http://www.asc-csa.gc.ca/eng/satellites/radarsat1/default.asp). Therefore, ice analysts cannot rely on SAR imagery alone and often use other remote sensing data such as visible and infrared imagery. It should be noted that the recent charts from many ice services are not completely independent of passive microwave data, although its relatively low-resolution imagery is usually only used as a last resort (occasions for its use have decreased with time as the number of alternative sources has grown [*National Ice Center*, 2006; *The Joint WMO-IOC Technical Commission for Oceanography and Marine Meteorology*, 2008]).

Due to the manual analysis method employed, the spatial variability within each chart is always low (relative to a passive microwave concentration product) and total concentration values (or ranges) are given in tenths. There is also a degree of subjectivity in the production of the charts, and focus is given to the marginal ice zone (where vessels are most likely to navigate). While it might be expected that, in preparing their charts ice analysts would overestimate the position of the ice edge to reduce danger to shipping, we found no evidence to suggest this is the case from detailed discussions of working practices and procedures at the Ice Analysts Workshop [*The Joint WMO-IOC Technical Commission for Oceanography and Marine Meteorology*, 2008]. The use of different ice analysts may have also resulted in inconsistencies through time. It should be noted that the charts are not reproducible, due to the manual method employed and because the imagery that they are based on are not always archived. Despite these limitations, the main strength of the sea ice charts is that they make the most out of the multiple data sources that are available. They are an expert's best guess at the "true" state of the ice conditions.

2.2.1. National Ice Center Sea Ice Charts

The National Ice Center (NIC), based in the U.S., has produced sea ice charts for the Arctic since 1972 and for the Antarctic since 1973. Early analyses were reliant on infrared, visible, and single-channel passive microwave imagery alongside some aerial reconnaissance data, with the use of in situ observations from ships for verification when possible. To provide complete hemispheric coverage, analysts often had to make educated guesses of the ice coverage in the 1970s, as data were not always available [*National Ice Center*, 2006]. Charts were hand drawn until 1995 and were output weekly until 2001 when production dropped to biweekly. NIC sea ice charts were usually based on data that were up to 72 h old. Older data have sometimes been used but adjusted using model guidance [*National Ice Center*, 2006]. Although the NIC charts are based on data assembled over several days, the ice analysts project the information forward to create a chart valid for a given day [*Fetterer*, 2006; *Dedrick et al*., 2001].

Arctic NIC sea ice charts are available on the National Snow and Ice Data Center (NSIDC) website in gridded digital format [*National Ice Center*, 2006]. This data set currently contains concentrations from when the ice charts began in 1972 through to 2007 on a 25 km EASE grid. Unfortunately, data south of 45°N are excluded from the product even though ice can often extend further south than this in the Gulf of St. Lawrence, the Sea of Okhotsk, and the Sea of Japan/East Sea.

Gridded NIC data for the Antarctic are not readily available. In 1996, the National Climate Data Center and NSIDC distributed a CD-ROM containing Arctic and Antarctic NIC chart concentrations for 1972 to 1994

[*National Ice Center, Fleet Numerical Meteorology and Oceanography Detachment, and National Climatic Data Center*, 1996]. NSIDC became aware of errors in the partial concentrations (concentrations for different ice types within a given area) on this product in 1997 and subsequently withdrew it. Here we use only the total concentrations (i.e., concentrations for all types of ice combined) for the Antarctic from this data set, which are available from 1973 until 1994 on a regular 0.25° longitude by 0.25° latitude grid. Shapefiles containing concentrations for some more recent years are available on the NIC website (http://www.natice.noaa.gov). The files provided for 2003 to 2007 have been obtained from the NIC website and gridded onto a 25 km EASE grid for use in this study. For both sets of Antarctic NIC chart data, the mean was taken when a concentration range was given (e.g., 90% is used for 8–10/10th). This is consistent with the gridded NIC chart data for the Arctic provided by NSIDC, already provided by them as mean values.

Current reporting practice is for the NIC ice analysts to mark the central ice pack as 9–10/10th, resulting in a concentration of 95%. However, this was not always the case and between the years of 1976 and 1986 convention was to use 10/10th (100%). This introduces an artificial discontinuity within the time series of concentrations [*Partington et al*., 2003]. For this reason we initially set all values of 95% to 100% in the NIC gridded data for both hemispheres but revisit this later in section 3.

It has been estimated that at best the present-day NIC ice chart concentrations have an uncertainty of 10% for values below 80% and an uncertainty $<$10% for values of 80% and above between the seasons of autumn and spring [*The Joint WMO-IOC Technical Commission for Oceanography and Marine Meteorology*, 2008]. In the summer the uncertainties increase to 30% and $<$20%, respectively. These values are based on charts that are derived using the best available data sources, in particular when high-resolution SAR imagery is available. The uncertainties would otherwise be larger.

As the OSI SAF passive microwave data were used as the primary source of data in HadISST.2.1.0.0 and due to the drawbacks highlighted in section 2.2, the NIC charts were only used directly in the construction of the data set in the absence of OSI SAF data, during the period from 1972/1973 to November 1978. However, the data after this period were used for comparisons and adjustments (Figure 1; see later in section 3 for details).

2.3. Walsh and Chapman Arctic Compilation

Walsh and Chapman have developed a data set containing Arctic sea ice concentrations [*Walsh*, 1978; *Walsh and Johnson*, 1978; *Chapman and Walsh*, 1991; *Walsh and Chapman*, 2001]. It contains a compilation of many different historical sources such as sea ice charts (see section 2.2) and reports, dating back to 1901. For HadISST.2.1.0.0 we used the same data as were used for HadISST1.1. End of month values on a regular 1° longitude by 1° latitude grid were provided by John Walsh.

Data prior to 1953 are primarily based on April to August ice edges from ice charts within Danish Meteorological Institute (DMI) annual reports, which were originally digitized by *Kelly* [1979]. The ice edges were based on a mixture of observations, extrapolation, and climatology. Walsh and Chapman inferred concentrations within the marginal ice zone using an average relationship between concentration and distance from the ice edge, based on passive microwave data. These values only vary seasonally, not regionally, and all values within the central pack have been set to 100%. September to March Walsh and Chapman data are mainly based on climatology, although the anomalies from the summer months were used to give some temporal variability [*Walsh*, 1978; *Walsh and Johnson*, 1978; *Chapman and Walsh*, 1991; *Walsh and Chapman*, 2001].

Data from 1953 to 1971 contain a number of sources. Walsh and Chapman did not attempt to adjust these sources for relative biases between them; therefore, the record is heterogeneous in time and space. The Walsh and Chapman data set also contains NIC sea ice charts (section 2.2.1) and passive microwave data (section 2.1), but we do not make use of the data set after 1972 (when the Arctic NIC sea ice charts began).

2.4. Antarctic Atlas Climatologies

Very few sea ice data are readily available for the Antarctic prior to 1973, when the Antarctic NIC sea ice charts began to be produced (section 2.2.1). We make use of two sets of seasonal ice edge climatologies, which were based on ice charts found in atlases and cover two different periods. The first of these climatologies is from a German ice atlas [*Deutsches Hydrographisches Institute*, 1950] and covers the period 1929 to 1939.

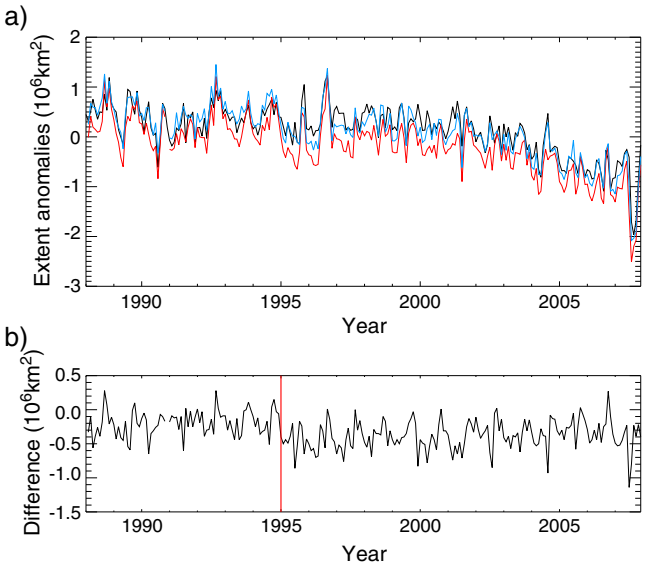

Figure 2. (a) Time series of Northern Hemisphere sea ice extent anomalies (relative to the NIC chart monthly climatologies for 1995–2007), 1988–2007, for the NIC chart data (black), subsampled OSI SAF data (red), and the adjusted subsampled OSI SAF (blue). (b) Subsampled OSI SAF minus NIC chart difference series. Red vertical line indicates where a discontinuity is seen at the start of 1995.

The second climatology is from a Russian Antarctic atlas [*Tolstikov*, 1966] and covers the period 1947 to 1962. Both of these ice edge climatologies were originally digitized onto a 1° longitude by 1° latitude grid for use in the Global sea Ice and SST data set [*Parker et al*., 1995; *Rayner et al*., 1996].

3. Data Set Construction

It was vital that the concentrations from the different data sources were made consistent in time and space before they were merged together, so that no artificial discontinuities were introduced into the record. Bias adjustments were required for this, and comparisons during periods of overlaps were made. We began with a comparison of OSI SAF and NIC chart sea ice extent anomalies in the Northern Hemisphere (NH) (Figure 2). Monthly mean concentrations for the SSM/I period (1988 to 2007) were calculated from (i) the OSI SAF daily data using a subset of days corresponding to the days for which the weekly/biweekly NIC Charts were valid (herein referred to as the "temporally subsampled" OSI SAF data) and (ii) the NIC chart data, for a like for like comparison. The temporally subsampled OSI SAF data were also converted from a 12.5 km EASE grid to a 25 km EASE grid to match the NIC chart resolution. Extents are calculated from the total area of ocean grid boxes containing at least 15% ice and are often used for monitoring hemispheric or regional sea ice trends. They were calculated using only the grid boxes that were not designated as land in either source, to remove any differences resulting from different land/sea masking. Anomalies were calculated relative to the 1995 to 2007 NIC chart monthly climatologies.

Figure 2 (top) shows that the NIC chart extents (black) are generally larger than the temporally subsampled OSI SAF extents (red). It can also be seen that a discontinuity occurs in the NIC chart extents in 1995 compared to the OSI SAF extents, which is particularly noticeable in the difference series (Figure 2, bottom). This coincides with the advent of high-resolution satellite imagery, such as SAR, and the change from hand-drawn to digital charts (section 2.2). The NIC chart record appears stable relative to OSI SAF after this time; therefore, we chose to use the NIC chart data from 1995 onward as the representation of the "true state" against which to adjust the relative biases in the other data sources used. It was necessary to adjust the data relative to one data source to achieve an internally consistent record. Even with its drawbacks, NIC chart data (section 2.2.1) was our only option, given the known problems of passive microwave data (section 2.1) and the cost and complexity of SAR imagery interpretation (section 2.2). Information from the latter is included within the ice charts, albeit with use of other sources when SAR imagery was not available. The decision to use any one particular source as a reference affects the average concentrations and extents throughout the record. If we

were to choose another reference, it would cause our data set to consistently provide larger or smaller concentrations (and extents/area), depending on the choice.

Unfortunately, there are no Southern Hemisphere (SH) NIC chart data available for the period 1995 to 2002 (section 2.2.1), so we only use the years 2003 to 2007 as our reference here.

Arctic and Antarctic bias adjustments were derived independently. In general, we cascade our adjustments for relative biases between sources backward in time using overlap periods. First we applied bias adjustments to the most recent data (OSI SAF, as given by the red line in Figure 1) relative to our chosen reference (NIC chart data for 1995 to 2007 for the NH and 2003 to 2007 for the SH, as given by the purple lines in Figure 1). The method used for the bias adjustments is described in section 3.1, using OSI SAF NH data as an example. We then adjusted the NIC chart data prior to November 1978 (solid blue lines in Figure 1). This required both temporal sampling adjustments (using the daily unadjusted OSI SAF data) to account for the weekly subsampling of the charts as well as bias adjustments, using the 1979 to 1994 overlap between the NIC chart monthly means (dashed blue lines in Figure 1) and the bias-adjusted OSI SAF monthly means. Full details of the OSI SAF and NIC chart temporal and bias adjustments are given in section 3.2. We then focussed on the earlier data. A method to estimate concentrations given an ice edge was necessary for the historical fields prior to the early 1970s and is outlined in section 3.3. Section 3.4 describes the processing of the Walsh and Chapman data for the Northern Hemisphere prior to 1972 (green line in Figure 1), and section 3.5 describes the processing of the Atlas climatologies for the Antarctic prior to 1973 (orange lines in Figure 1). Finally, the completion of the global record is described in section 3.6, where the multiple data sources were combined into a 1° longitude by 1° latitude grid.

3.1. Bias and Temporal Sampling Adjustment Method

This section describes the method used to adjust for biases in the input data relative to our chosen representation of the "true state". This method was also used to adjust for the effect of incomplete temporal sampling in the NIC charts (when using weekly/biweekly data rather than daily data to calculate monthly means). We illustrate the method using the example of the OSI SAF NH bias adjustments, which were calculated relative to the post 1995 NIC chart data for each calendar month. Figure 3 shows a scatterplot comparing temporally subsampled OSI SAF monthly means to the NIC chart monthly means for each grid box for January and July. Clustering can be seen around the nearest 5% in the NIC chart values as the original concentrations were given to the nearest 5 or 10%. Other values can also be seen as we have used monthly means. The majority of points lie above the 1:1 line, indicating that the NIC chart monthly mean concentrations are generally higher than those of the OSI SAF in both winter and summer months. The OSI SAF values were binned using 1% bins centered on whole values from 1% to 100%. A bootstrap method was then used to randomly sample the corresponding NIC chart values within each bin 100,000 times (regardless of the size of the original population, which could be larger or smaller than 100,000). Medians were then calculated from the population of 100,000 NIC chart values for each bin. These provided a bias-adjusted value for each calendar month applicable to each original OSI SAF monthly mean concentration. Where necessary, the bias-adjusted values were linearly interpolated between the central values of each bin, as given by the red lines in Figure 3.

Our initial concern about this method when applied to the OSI SAF data was that the very high values were dictated by the discrete nature of the NIC chart data. This caused all the high concentrations to be arbitrarily set to 100%. It is unlikely that the actual concentrations are quite this high within much of the central pack, as leads (cracks within the ice) often form as the ice moves about. We therefore linearly interpolated between the point at which the adjustment values reach 95% and the point at which both the original concentration and the adjustment value is 100%, as given by the green line in Figure 3. This retains the original spatial variability of the passive microwave data while being consistent with the uncertainty in the NIC chart data (many NIC concentrations within the central pack were originally set to 9–10/10th; see section 2.2.1). This step was only employed during the OSI SAF NH and SH bias adjustments, as it was not deemed necessary for the NIC chart temporal sampling and bias adjustments (section 3.2).

We adjust the temporally subsampled OSI SAF data to check the effect of the adjustments on the concentrations and extents. It can be seen from Figure 2 that the extents calculated from the bias-adjusted subsampled OSI SAF concentrations (blue) agree much better with the extents from the post-1995 NIC chart data than do the unadjusted data. Figure 4 shows the mean fields for July. It should be remembered when comparing mean fields such as these (and others within this study) that they represent the mean conditions

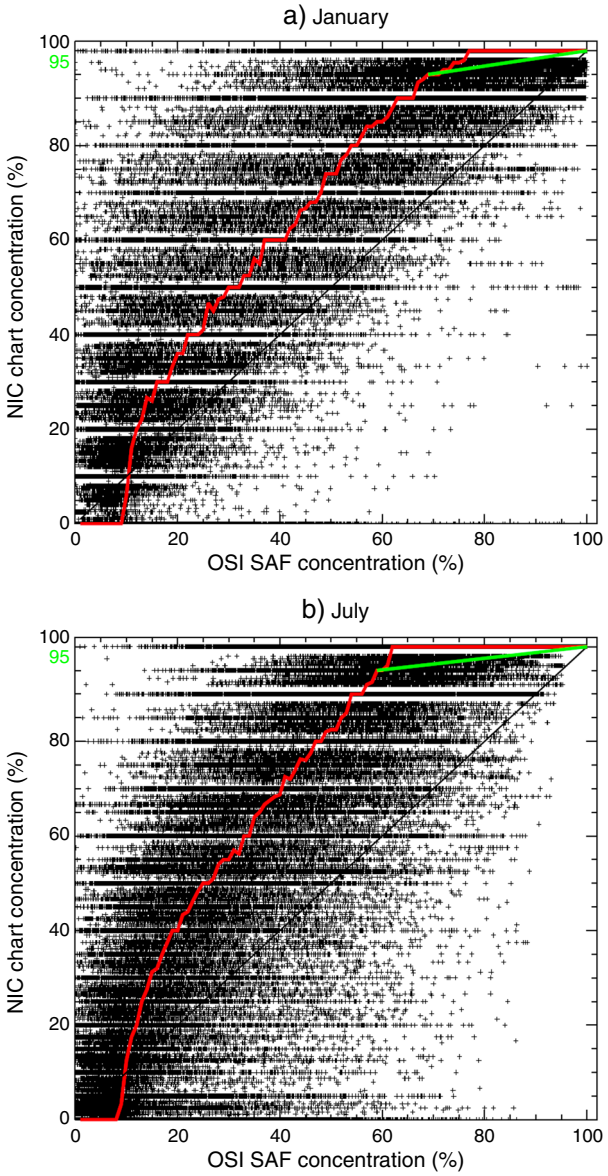

Figure 3. Scatterplots for (a) January and (b) July showing the monthly mean sea ice concentrations in the Northern Hemisphere NIC charts plotted against the OSI SAF retrievals for all corresponding grid boxes. The 1:1 line is given by the black diagonal line. Median values calculated from a bootstrap approach provided a set of adjusted OSI SAF values (red line). Adjusted values above 95% were linearly interpolated between 95 and 100% (green line).

whose distribution of concentrations differs from the distribution in individual fields. Often, much larger areas of the low to middle concentrations can be seen in the mean fields, compared to those seen in individual fields, due to the interannual variability of the monthly fields. Concentration differences between individual fields from different data sources are usually much larger than those seen in mean fields too, and vary greatly from month to month. The mean fields do, however, give an overall picture of the concentrations and the differences. Figure 4 shows that the mean bias-adjusted concentrations agree much better with the NIC charts than the mean unadjusted data. The concentrations within the central pack are seen to be a little lower, but this is to be expected due to the way we adjust concentrations over 95%.

3.2. OSI SAF and NIC Processing

Monthly means were calculated using all available NH and SH OSI SAF data (i.e., using all available days within each month) on a 12.5 km EASE grid to give "fully sampled" monthly concentrations. All values of concentrations,

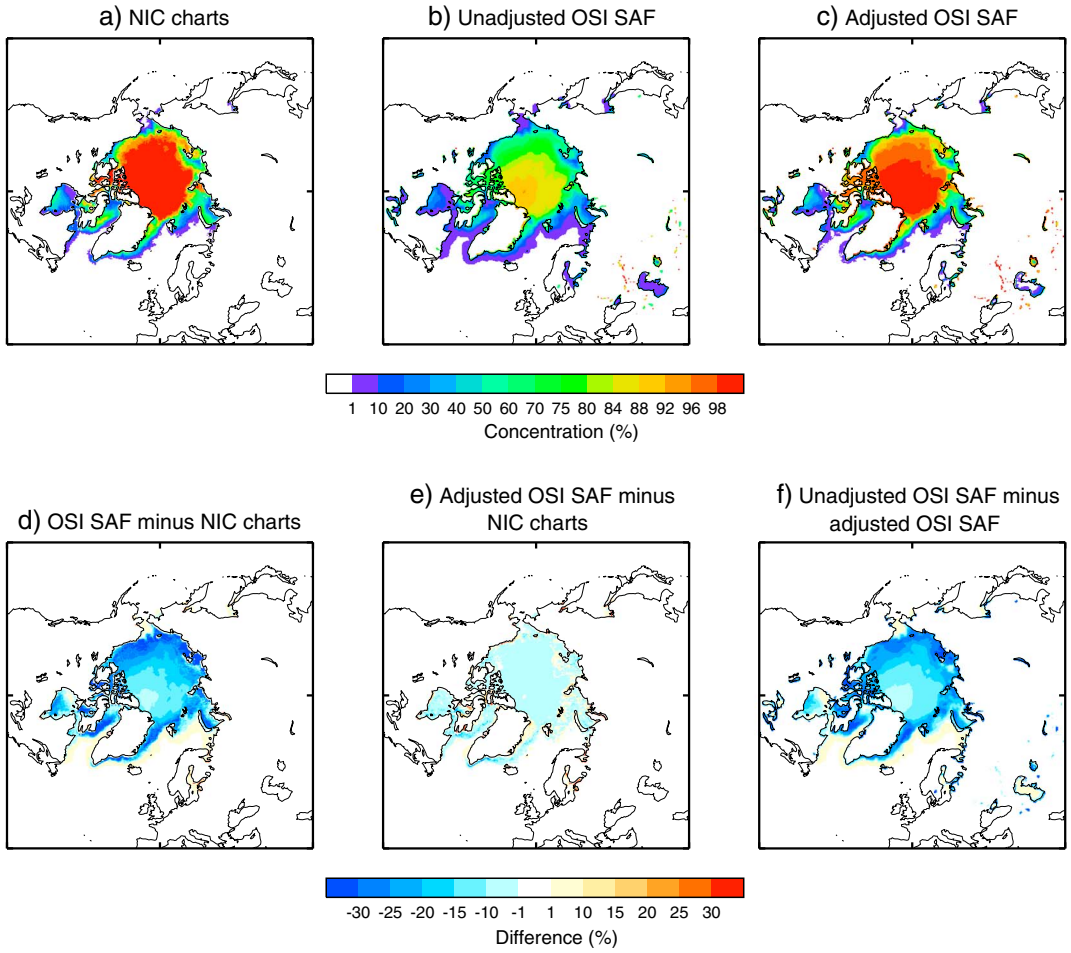

Figure 4. (top row) Mean sea ice concentration fields for July, 1995–2007 for (a) the NIC chart data; (b) the unadjusted subsampled OSI SAF data; and (c) the adjusted subsampled OSI SAF data. (bottom row) Differences in the mean fields for (d) the unadjusted subsampled OSI SAF minus NIC chart data; (e) the adjusted subsampled OSI SAF minus NIC chart data; and (f) the unadjusted minus adjusted subsampled OSI SAF data.

however small, were retained for each data source until the final stages of the data set construction (section 3.6). The NH adjustments calculated in section 3.1 were then applied to the set of fully sampled NH monthly means. SH adjustments were also separately calculated using the same method, using OSI SAF monthly means calculated from temporally subsampled daily data (based on the NIC chart dates) on a 25 km grid for 2003 to 2007 (as no data for 1995 to 2002 were available), and NIC chart monthly means for the same period. These were then applied to the fully sampled SH OSI SAF monthly means on a 12.5 km grid as for the NH.

Figure 5 compares the mean OSI SAF fields for January and July in the Arctic before and after the adjustments. It can be seen that the largest adjustments are applied to the medium values of concentrations toward the edge of the ice. Overall the adjustments have a much larger effect during the summer months. This is due to both the larger bias adjustments that were calculated for most given values of concentration (Figure 3) as well as the extensive regions of high concentrations within the central pack that were underestimated in the summer. This is a well-known problem with passive microwave retrievals and is due to melt ponds that form on top of the ice during the melting season [*Inoue et al.*, 2008; *Andersen et al.*, 2007]. The winter OSI SAF fields consist mainly of very high concentrations (above 95%) within the central pack, and these values only require relatively small bias adjustments. In the Antarctic (Figure 6) the bias adjustments are also seen to increase the OSI SAF values throughout the year, particularly during November (not shown) and December, due to the underestimation of the passive microwave concentrations compared to the NIC ice charts. This is possibly due to the presence of thin ice or surface conditions (such as snow), which are also known to cause underestimates in passive microwave retrievals [*Shokr and Kaleschke*, 2012].

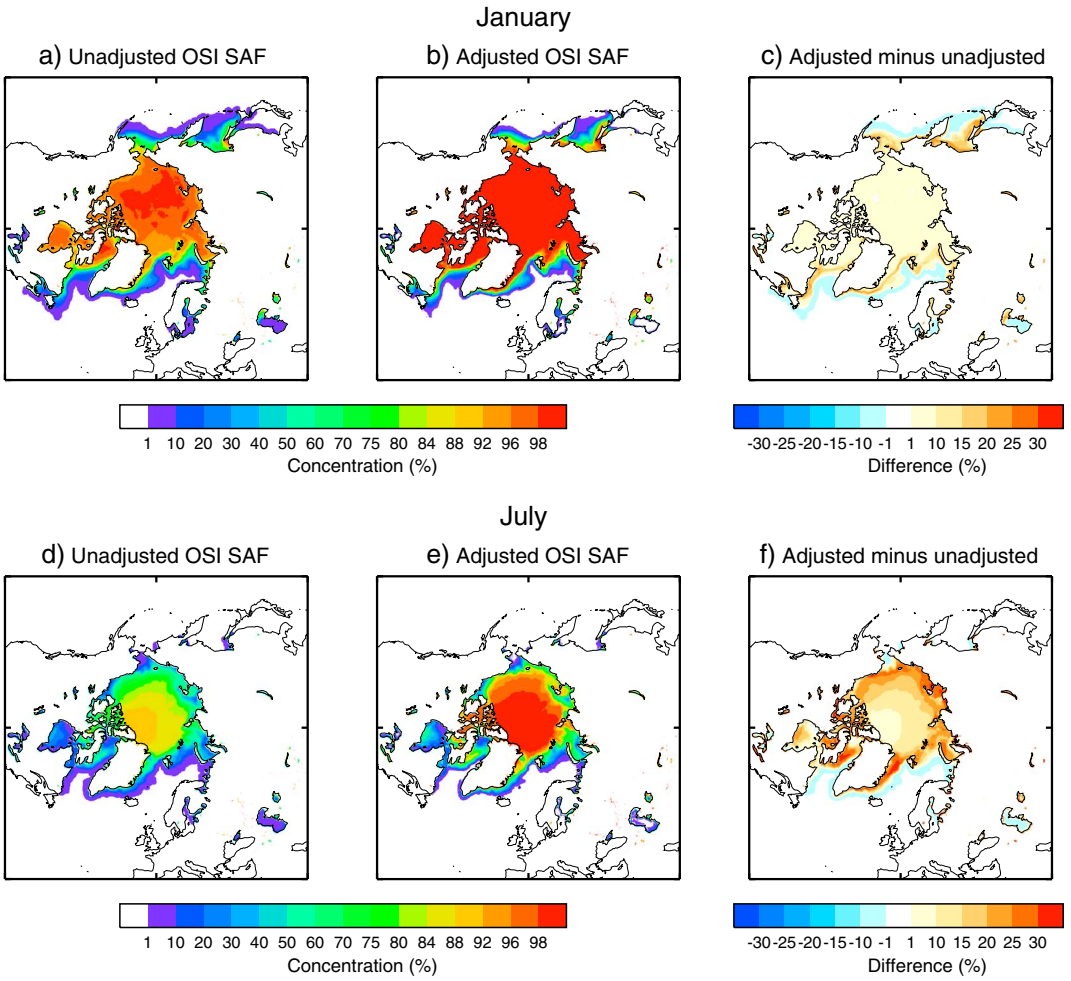

Figure 5. Northern Hemisphere mean sea ice concentration fields and differences, 1979–2007, for (top row) January and (bottom row) July. Mean concentrations are given for (a and d) the unadjusted OSI SAF data and (b and e) the adjusted OSI SAF data. (c and f) Differences in the mean fields.

Next we focussed on the NIC chart data prior to the start of the OSI SAF passive microwave record (1972 to October 1978 for the NH and 1973 to October 1978 for the SH). To make the NIC data consistent with the fully sampled bias-adjusted OSI SAF data, we first calculated temporal sampling adjustments to quantify the effect of the weekly resolution of the charts on the monthly means calculated from them. This was done by comparing OSI SAF monthly means calculated from weekly resolution data to fully sampled OSI SAF monthly means (calculated from all available daily resolution data). We used the unadjusted OSI SAF data throughout the daily SSM/I period of the passive microwave record (July 1987 to 2007) to do this, as we have only bias adjusted the monthly means and not the daily fields. As the weekly NIC chart dates for each month have varied from year to year, it was necessary to calculate a different set of temporal adjustments for each month within the 1972/1973 to October 1978 period (for each hemisphere). The weekly chart dates for each month were used to calculate temporally subsampled monthly means from the daily unadjusted OSI SAF data for the same calendar month throughout the period. For example, in 1972 NH charts were available for 3, 10, 17, 24, and 31 January. We calculated January temporally subsampled OSI SAF monthly means using the same dates within each January between 1988 and 2007. We then calculated a set of adjustments for January 1972, using the January temporally subsampled OSI SAF monthly means and the method described in section 3.1, with the corresponding fully sampled unadjusted OSI SAF means for January as the reference data set. The temporal adjusted values above 95% were not reset linearly between 95% and 100%, as was done for the OSI SAF bias-adjusted values. Each set of temporal adjustments was applied to the NIC chart monthly mean field for the corresponding month and hemisphere.

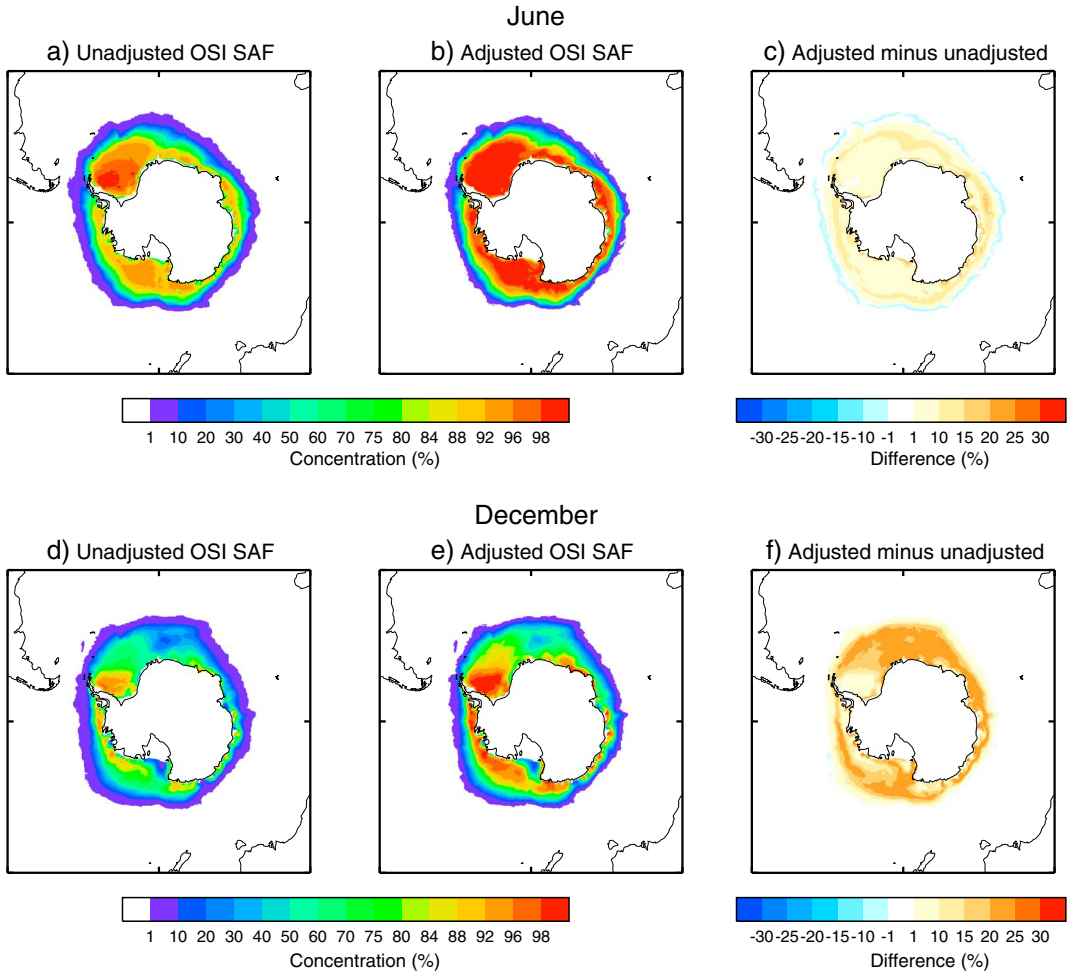

Figure 6. As Figure 5 but for (a–c) June and (d–f) December in the Southern Hemisphere.

Following the NIC chart temporal sampling adjustments, bias adjustments were also required relative to the fully sampled bias-adjusted OSI SAF data. We used the overlap period of 1979 to 1994 to do this for both hemispheres. This assumes that the NIC chart data prior to November 1978 is broadly consistent with the NIC chart data for 1979 to 1994. As the early NIC chart data in the SH were on a 0.25° grid, we converted the fully sampled bias-adjusted OSI SAF data from a 12.5 km EASE grid to a 0.25° grid before the bias adjustments were calculated. In the NH the fully sampled bias-adjusted OSI SAF data were simply reduced from 12.5 km to 25 km EASE grid resolution. The method described in section 3.1 was used to calculate bias adjustments for the temporally adjusted NIC data relative to the fully sampled bias-adjusted OSI SAF data. Again, NIC chart bias-adjusted values above 95% were not reset linearly between 95% and 100%, as was done for the OSI SAF bias adjustments. Due to the nature of the NIC chart data (original concentrations were given to the nearest 5 or 10%), a bin size of 5% was used. We use bias-adjusted NIC chart data for each hemisphere prior to November 1978, when the OSI SAF record begins.

3.3. Method to Estimate Concentrations Based on the Ice Edge

A method to estimate the concentrations within the pack from the ice edge was needed so that we could make use of data where only ice extent was available. This was done using the bias-adjusted OSI SAF data to calculate a set of estimated concentration values along each 1° longitude band for each hemisphere, based on the distance to the ice edge (open water). In this section we describe the method used (which we apply to the Walsh and Chapman data in section 3.4 and the Atlas climatologies in section 3.5). We also discuss how the estimated values were applied to the original bias-adjusted OSI SAF ice edges to check the estimated concentration fields against the original concentration fields.

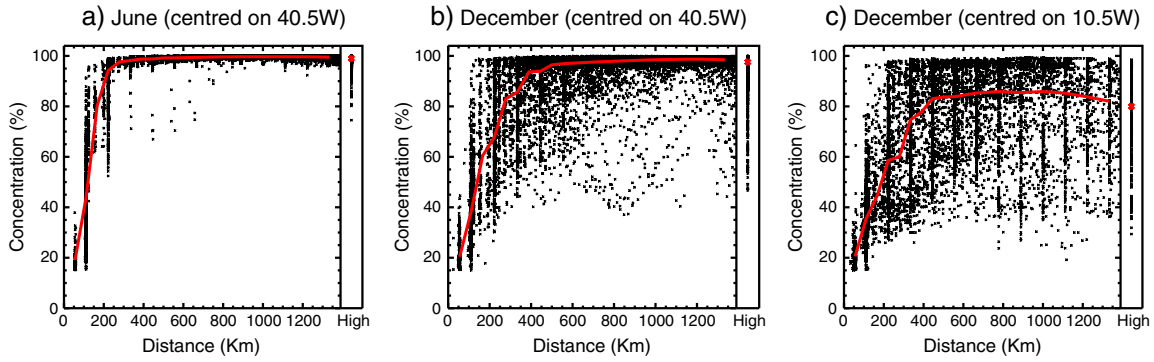

Figure 7. Scatterplots showing the Southern Hemisphere monthly mean grid box concentrations for a given 21° longitude section against the closest distance to the ice edge. (b) The scatterplot for December concentrations centered on 40.5°W is compared to (a) the scatterplot for the same location but for June and (c) the scatterplot for the same month but centered on 10.5°W.

The final globally complete fields on a 1° latitude by 1° longitude grid (section 3.6, but excluding data in the Great Lakes and Caspian Sea) for 1979 to 2007, based on the bias-adjusted OSI SAF data, were used to estimate the relationship between concentration and distance to the ice edge. For each grid box in the adjusted OSI SAF data that contained an ice concentration we calculated the distance to the center of the nearest grid box that contained open water (0% concentration) to give the distance from the ice edge. For each 1° longitude band we selected all the points from 10° longitude either side (giving a 21° longitude band) to produce a scatterplot of concentrations against the distance from the ice edge. We used a very similar method to the bias adjustment method described in section 3.1 to produce a set of estimated concentration values based on the distance to the ice edge. Distances were binned using a bin size equal to the distance of 0.5° latitude (approximately 55.6 km), centered on multiples of the same value, up until the tenth bin (centered on approximately 556.0 km). For distances greater than this, a bin size equal to the distance of 1° latitude was used until the seventeenth bin (centered on approximately 1334.4 km). All longer distances were binned into a "high" bin to yield one concentration that represents the very center of the pack. A median concentration for each bin was calculated if at least 20 values were available in the bin.

As before, we used a bootstrap method to calculate medians from a population of 100,000 that were randomly sampled from the corresponding adjusted passive microwave concentrations within each bin. These provided a set of estimated concentrations for a given longitude that could be applied to a grid box according to its distance from the ice edge. The estimated concentrations were linearly interpolated between the center of each bin (including between values where missing bins were found), as given by the red curve in Figure 7. For distances that were smaller than the first bin (or if this was missing then the next lowest bin where a value had been calculated), the interpolation was calculated between 15% (which was assumed to be the very edge of the ice) and the concentration given by the first (or lowest) bin. The exception to this was when the bins closest to the water were missing and the lowest bin available contained a concentration of 90% or greater. This occurred at longitudes where any ice was consistently at a long distance from open water during the passive microwave period (e.g., north of Siberia in autumn to spring). To allow for any regions in the historical charts that may have had less extensive ice cover than in the passive microwave period (i.e., where open water is found close to these regions) an average marginal ice zone for each month was calculated using the average distance of the 90% ice concentration contour from the edge of the ice. If the grid box lay within this average marginal ice zone distance, then we linearly interpolated between 15% (again, assumed to be the edge of the ice) and the concentration found in the lowest bin containing data (which is assumed to be the concentration at the point equal to the average marginal ice zone distance). The estimated concentration from the high bin was used for distances that were larger than the central value of the 17th bin. If a high concentration value was not calculated due to lack of data, then the highest bin containing an estimated concentration was used for all distances larger than the central value of the bin.

It was necessary to use a larger bin size for the furthest distances as there were often fewer data points available within each bin. There was also very little difference between the values calculated from each bin as they usually contained the very high concentrations within the central pack. Conversely, a smaller bin size

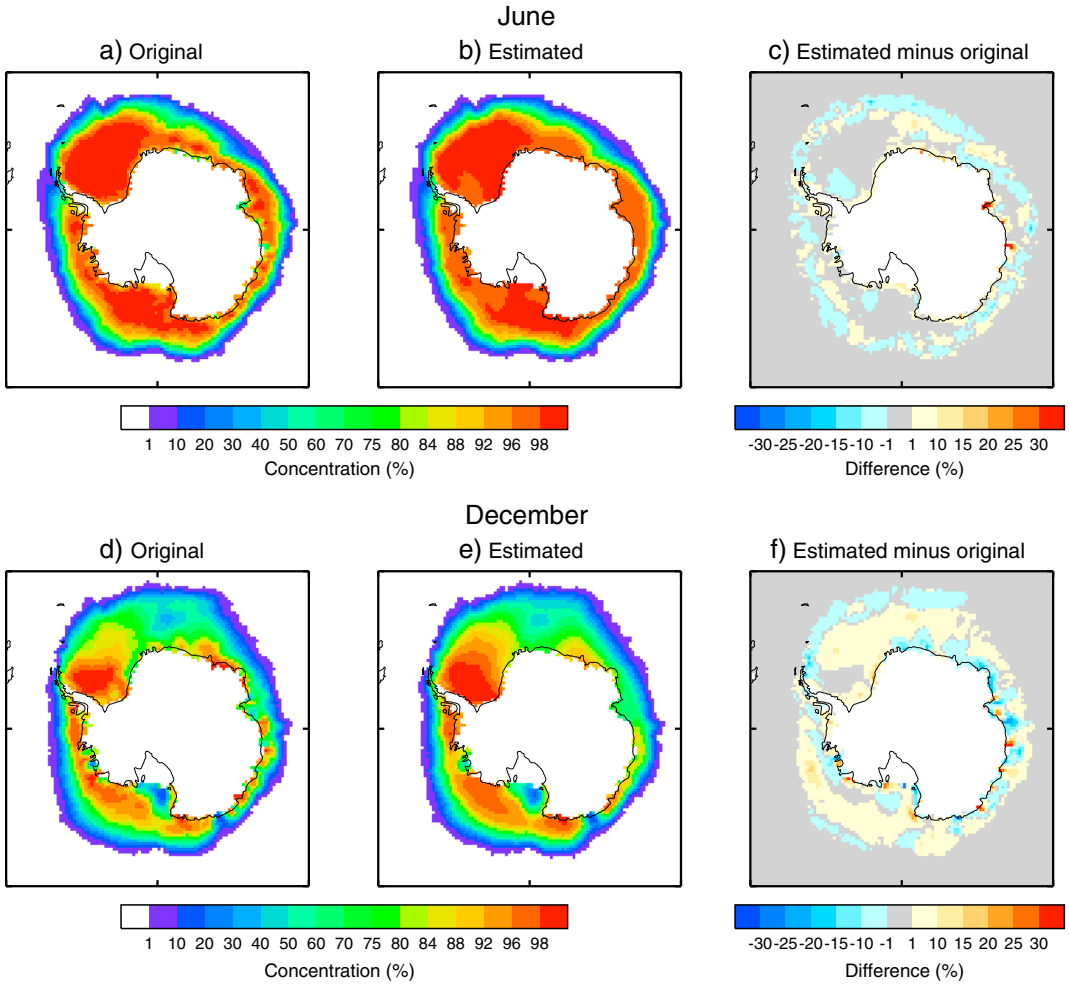

Figure 8. Southern Hemisphere mean concentration fields and differences, 1979–2007, for (top row) June and (bottom row) December. Mean values are given for (a and d) the original OSI SAF data and (b and e) concentrations estimated from the OSI SAF ice edge positions. (c and f) Differences in the mean fields.

was required for the distances nearest to the ice edge to accurately represent the sharp gradient of concentrations within the marginal ice zone.

Figure 7 compares the scatterplot for December in the SH, for the 21° longitude band centered on 40.5°W (center), with the scatterplot for the same location but for June (left), and the scatterplot for the same month but centered on 10.5°W (right). It can be seen that the marginal ice zone is much narrower in the winter (June) with concentrations that increase poleward at a much higher rate. The results vary greatly with longitude; for example, it can be seen in Figure 7 that the concentrations increase at a lower rate further east (at 10.5°W) in December and the concentrations far poleward of the ice edge are much lower.

The method was checked by applying the technique to passive microwave extents and comparing the estimated concentrations to the original concentrations. Figure 8 compares the mean concentration fields for the Antarctic in 1979 to 2007 for the original adjusted OSI SAF data and the estimated fields (constructed from the adjusted OSI SAF ice edges). The mean fields are broadly consistent, although the differences are larger for individual fields due to the limited spatial variability we can estimate when only an ice edge is provided.

3.4. Walsh and Chapman Processing

As the Walsh and Chapman data set contains end of month sea ice concentrations, it was necessary to apply temporal adjustments to convert to values that represent the monthly means. We used the OSI SAF record, on the 1° longitude by 1° latitude Walsh and Chapman grid, to calculate 15 year climatologies based on both

the end of month values (taken from the last day of each month) and the monthly means from 1979 to 1993. End of month anomalies were calculated by subtracting the end of month climatology from the Walsh and Chapman data set from January 1901 to December 1971. For each month these grid box anomaly values were interpolated between the end of the previous month and the end of the month in question to produce midmonth anomalies, except for January 1901 which used the end of month anomalies for the same month. This set of anomalies was then added to the monthly mean climatology to give concentrations equivalent to the monthly means.

Due to the heterogeneous nature of the concentrations contained within the Walsh and Chapman data set, it was decided to only use the extents based on the temporally adjusted Walsh and Chapman data. Ideally, an attempt would have been made to retain observations of concentrations where they exist within the compilation, but the exact locations and times of these as well as the original source were unknown. Many of the Walsh and Chapman fields were originally based on extents, and concentrations were estimated by them using a simple method (section 2.3) yielding a few discrete values with little spatial variability and 100% throughout the central pack. Reestimating the concentrations using our more complex method that varies longitudinally as well as monthly (section 3.3) makes the distribution of concentrations within the fields consistent with the later part of the record and introduces higher spatial variability. This does assume that the Walsh and Chapman ice edge is representative of the 15% ice contour and that the extents do not require bias adjustment. It also assumes that the distribution of concentrations within the ice edge for the period 1901 to 1971 was broadly similar to that for the 1979 to 2007 period in the Arctic.

The Gulf of Saint Lawrence, Sea of Japan/East Sea, and Sea of Okhotsk were replaced with the 25 year monthly mean adjusted OSI SAF climatology there due to lack of data and irregular features in the extents. As for HadISST1, the Walsh and Chapman fields for 1940 to 1952 were reset to the calendar monthly climatologies calculated from the full (1940–1952) period. This originally seemed to consist of two very different unrealistic climatologies (not shown here; see *Rayner et al*. [2003, Figure 1g]). It was noted that a small area northeast of Greenland contained open water even though it was surrounded by ice throughout the record, so this was reset as ice. A monthly mean climatology was calculated from the fields from 1901 to 1930 and used for all years prior to this, beginning in 1850.

The distance from the ice edge was calculated for all grid boxes containing ice within the adjusted Walsh and Chapman data. Concentrations for these grid boxes were then estimated as described in section 3.3. Figure 9 compares some examples of the temporally adjusted Walsh and Chapman fields before and after the concentrations were reestimated. It can be seen that the newly estimated fields contain higher spatial variability and a shorter marginal ice zone (consistent with the adjusted OSI SAF data). There is a noticeable area of concentrations of around 90% in the original Walsh and Chapman field for July 1968 (Figure 9, bottom left). Although it could be argued that this may be a real feature based on ice charts/reports, the feature disappears in the fields in the following month (August 1968, not shown). During the melt season we would expect a feature such as this to persist. The disappearance may be due to biased observations in July (possibly due to a change in original data source) or lack of observations in August (due to the changing and unknown observational coverage throughout the series). However, by reestimating the concentrations, we have removed discontinuous features such as this (albeit perhaps at the expense of losing variability within the pack that is based on observations). This is important when trying to create a data set that is often used for providing a lower boundary forcing to atmospheric models, where sudden changes in sea ice concentration are undesirable.

3.5. Antarctic Atlas Processing

It was assumed that the Antarctic Atlas ice edge climatologies (section 2.4) represented the 15% sea ice concentration contour and that the distribution of concentrations within the ice edge prior to 1973 was broadly similar to that in the 1979 to 2007 period in the Antarctic. Concentrations were estimated for both climatologies using the method described in section 3.3. The concentration fields derived from the German Atlas climatology were used between 1929 and 1939 as well as for all years prior to this. The concentration fields derived from the Russian climatology were used from 1947 to 1962. Extents for the missing years between the two climatologies (1940–1946) and between the Russian climatology and the start of the NIC chart record (1963–1972) were calculated using simple linear interpolation in each grid box between the concentrations from the fields either side of the missing period. A 25 year climatology based on the adjusted NIC chart and OSI SAF data for 1972 to 1996 was calculated and used in the linear interpolation of the later

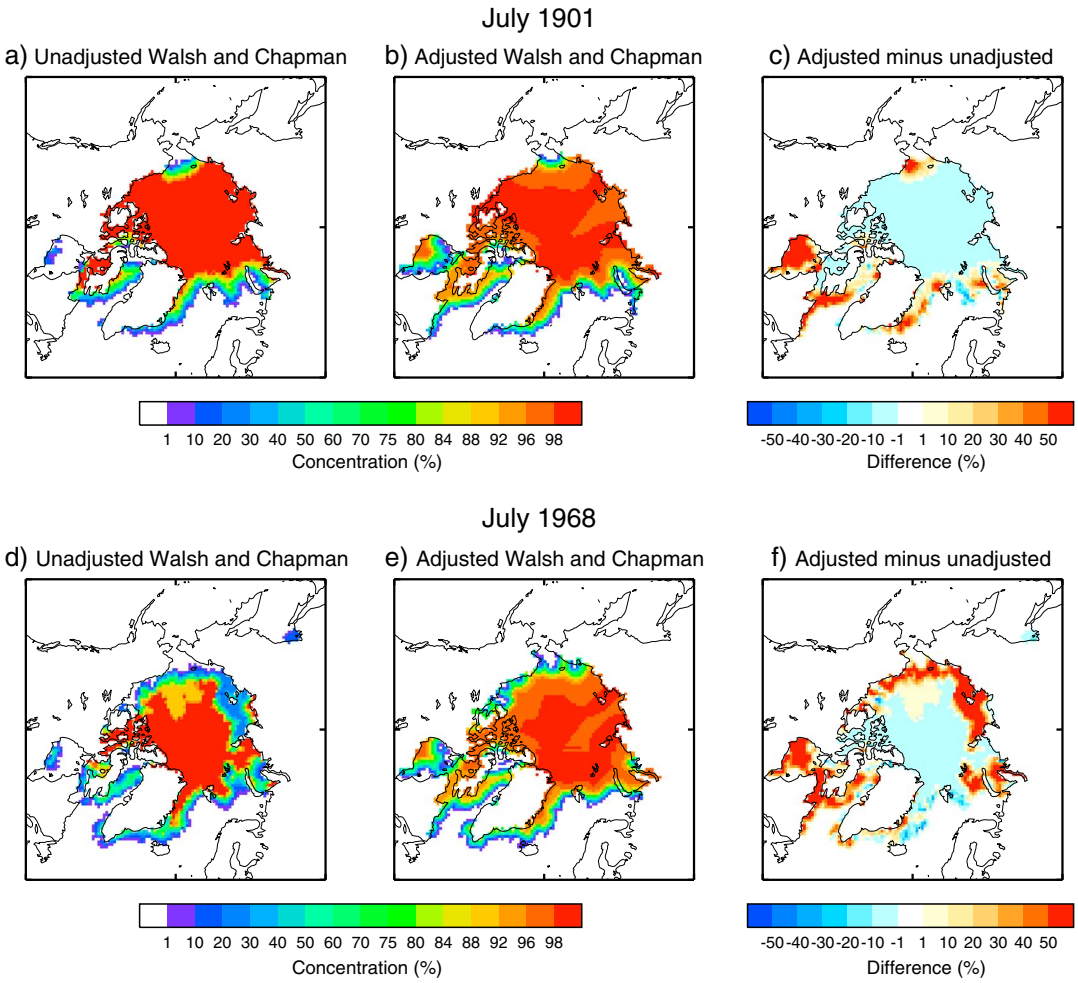

Figure 9. Northern Hemisphere concentration fields and differences for (top row) July 1901 and (bottom row) July 1968. (a and d) Walsh and Chapman data. (b and e) Concentrations estimated from the Walsh and Chapman ice edge positions. (c and f) Differences in the fields.

missing period. Concentrations for the missing periods were estimated from the linearly interpolated extents using the method described in section 3.3.

3.6. Completion of the Global Fields

The final stage of the data set construction was to combine all fields into a global data set. The adjusted OSI SAF NH and SH fields were reduced to a 25 km grid and then converted to a regular 0.25° grid along with the adjusted NIC chart fields for the NH. These were combined with the adjusted NIC chart data for the SH to create a complete global series of concentration fields for 1972 to 2007 (albeit with missing data in the Antarctic for 1972 due to the lack of NIC chart data then). All concentrations were converted from percentages to fractions (by dividing by 100) for consistency with HadISST1. Concentrations above 0.00 and less than 0.15 were reset to open water (0.00). A 0.25° land/sea mask was created so that a consistent mask could be applied throughout the data set and then applied to the global fields to remove any ice or open-water values around the coasts that were not required, and to highlight any ocean grid boxes that were missing data (excluding the Great Lakes and Caspian Sea which were set as missing at this stage). These were filled in using the mean of the nearest neighboring grid boxes.

The fields were then reduced to a regular 1° grid and combined with the infilled Walsh and Chapman concentration fields, as well as the Antarctic concentration fields prior to 1973 that were based on the Atlas climatologies (these were also converted from percentages to fractions). HadISST1 concentrations for the Great Lakes and Caspian Sea were used to fill in these regions, as they were either missing or deemed

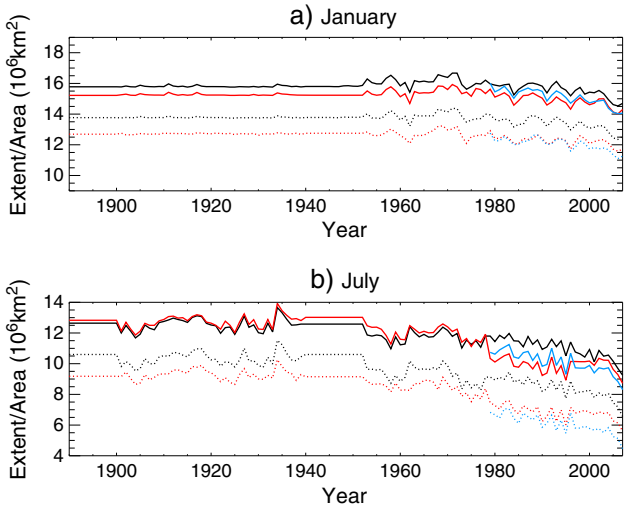

Figure 10. Time series of Northern Hemisphere sea ice extent (solid) and area (dotted), 1890–2007, for HadISST.2.1.0.0 (black), HadISST1.1 (red) and NASA Team (blue). Monthly mean values are shown for (a) January and (b) July.

unreliable (a visual comparison of passive microwave OSI SAF concentrations with sea ice charts for the Great Lakes showed very large differences such as the presence of ice in the OSI SAF data set in ice-free months as indicated by the ice charts).

The 0.25° land/sea mask was reduced to 1° and applied to the global 1° fields to again remove any ice or open-water values around the coasts that were classed as land and to fill in any remaining missing sea grid boxes using the mean of the nearest neighboring grid boxes. It was noted that some spurious ice concentration remained in the NH far south of the ice pack, which originated from the Walsh and Chapman data. An "open water" mask was therefore manually created (based on all data sources used in the construction of HadISST.2.1.0.0) to reset these values to 0. Finally, any remaining concentrations below 0.15 were also reset to 0. This gave our set of global concentration fields from 1850 to 2007 for HadISST.2.1.0.0.

4. Results

4.1. Northern Hemisphere

4.1.1. Comparison With HadISST1.1 and NASA Team Passive Microwave Retrievals

We begin our comparison of HadISST.2.1.0.0 to other data in the Northern Hemisphere. Figure 10 shows a time series of extents and area for both HadISST.2.1.0.0 and HadISST1.1 data sets since 1890, alongside those for monthly means derived from NSIDC's passive microwave data set [*Cavalieri et al.*, 1996] (http://nsidc.org/data/nsidc-0051.htm), which is based on the NASA Team algorithm (hereafter referred to as NASA Team). The NASA Team monthly values were converted from a 25 km polar stereographic grid to a regular 1° latitude by 1° longitude grid. We used the strict criterion that all three data sets must contain a value (sea ice concentration or open water) at any given grid box for it to be included in the calculation of extent or area. The only exception to this was for the hole at the NH pole in the calculation of the NASA Team extents. Due to the orbits of their polar orbiting satellites, passive microwave instruments are unable to view small regions around the pole. This results in a hole of missing data in all passive microwave sea ice products in the Arctic. In the OSI SAF product (and therefore in HadISST.2.1.0.0), concentrations here were estimated based on neighboring grid boxes. This was also done in the construction of HadISST1.1, whereas the polar hole remains missing in the NASA Team product. It was assumed that the polar hole contained ice in the calculation of the NASA Team extents. In the calculation of the area we set all three data sets as missing in the polar hole rather than estimate the concentrations in the NASA Team data ourselves. Extents are always larger than area as they contain the areas of water as well as ice within the 15% concentration contour; however, there will be a larger difference between the two measures here due to the way we treated the hole at the pole during our calculations. It should be noted that HadISST1.1 contains monthly medians rather than means like

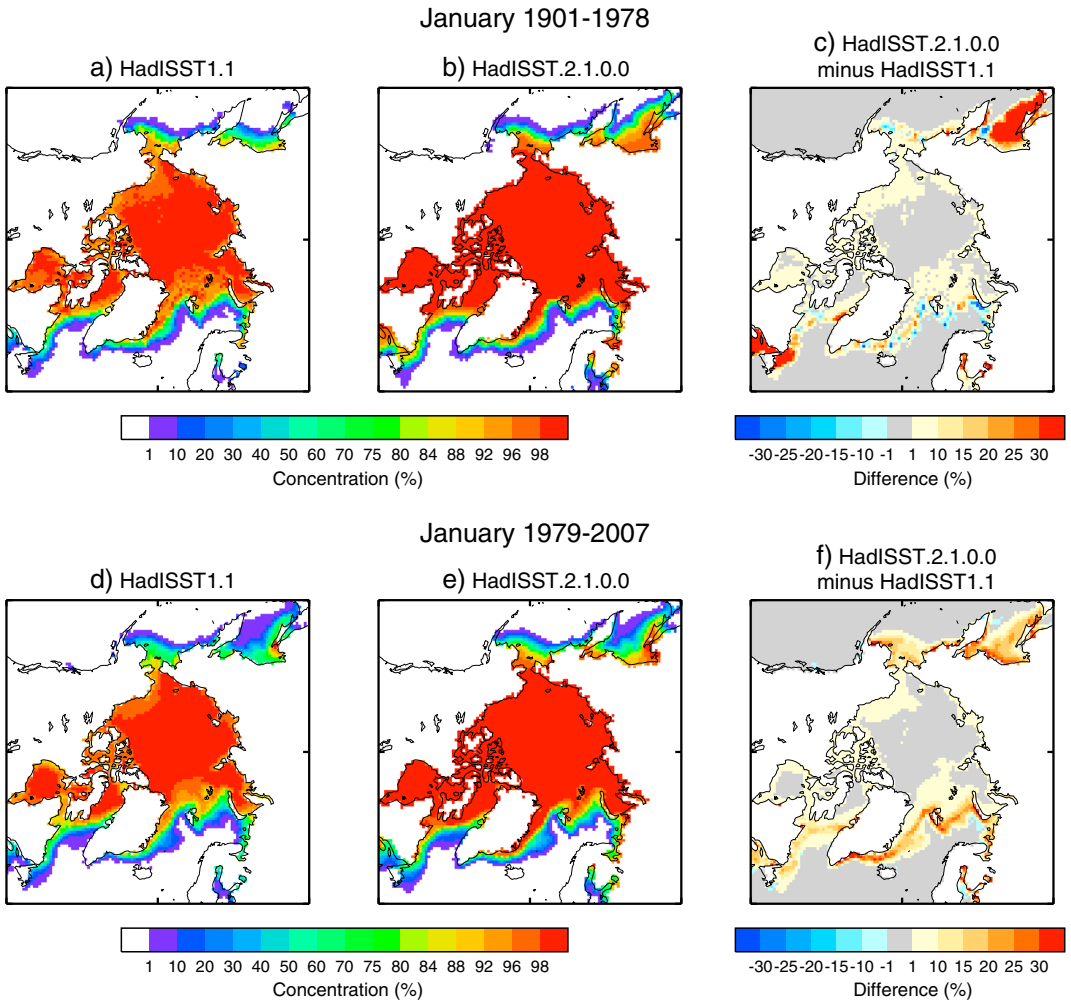

Figure 11. Northern Hemisphere mean sea ice concentration fields and differences in January for (top row) 1901–1978 and (bottom row) 1979–2007. Mean concentrations are given for (a and d) HadISST.2.1.0.0 and (b and e) HadISST1.1. (c and f) Differences in the mean fields.

HadISST.2.1.0.0 and NASA Team, which would be expected to result in a small relative offset in any calculations of area or extent.

It can be seen from Figure 10a that prior to 1953 the January time series of extent and area for both HadISST.2.1.0.0 and HadISST1.1 have very little variability, as the data for September to March then are primarily based on climatology (section 3.4). More variability can be seen from 1953 onward. HadISST.2.1.0.0 contains consistently larger extents and area than HadISST1.1 throughout the time series. The difference appears to be relatively consistent in time, which masks the two main underlying reasons for these differences. Figure 11 compares the mean fields for January from the two versions of HadISST and for two different periods: 1901 to 1978 and 1979 to 2007. For the earlier period it can be seen that HadISST.2.1.0.0 contains a lot more ice around the Sea of Okhotsk and the Gulf of Saint Lawrence compared to HadISST1.1. The Sea of Okhotsk was replaced with climatology in HadISST.2.1.0.0 (sections 3.2 and 3.4), whereas Walsh and Chapman data were used in HadISST1.1. Both versions used climatology in the Gulf of Saint Lawrence (except between 1972 and 1978 in HadISST.2.1.0.0, which is based on the NIC sea ice charts, section 3.2). In the later period, however, it can be seen that HadISST.2.1.0.0 is consistently a little more extensive around the perimeter of the ice edge than in HadISST1.1. It can also be seen for both periods that the concentrations within the pack are generally larger in HadISST.2.1.0.0, and there is a smaller marginal ice zone (i.e., the concentrations have a sharper gradient near the ice edge). This is reflected in the time series of area in Figure 10, which shows a larger difference between the two data sets than for the extents.

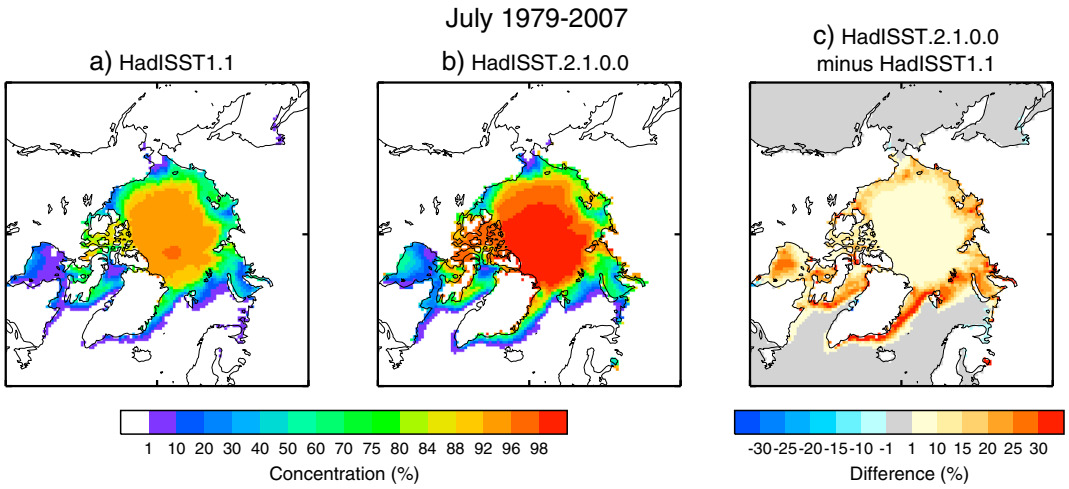

Figure 12. As in Figure 11 but for July 1979–2007 only.

Figure 10b shows that there is more variability in the time series of area and extents for both versions of HadISST in July between 1901 and 1938, compared to January. The period 1940 to 1952 is based on climatology (section 3.4). It should be noted that the years 1850 to 1889 have been excluded from Figure 10 as this period contains a monthly climatology that continues until 1900 (section 3.4). The extents for HadISST.2.1.0.0 are very similar to those for HadISST1.1 until the passive microwave record begins in 1979, when a large discontinuity in HadISST1.1 can be seen (this can also be seen in the area time series). The estimation and application of bias adjustments within this study has attempted to remove any discontinuity from HadISST.2.1.0.0 at this time, which occurs at a change in data source from NIC charts to OSI SAF passive microwave concentrations. A discontinuity can also be seen in HadISST1.1 in July at the start of 1997 (and also to a lesser extent in the time series for January, Figure 10a) when there was a change in passive microwave product used (section 1). A large difference can be seen between HadISST.2.1.0.0 and HadISST1.1 in the time series of area, even during the early period when the extents are similar. This is because the concentrations in HadISST.2.1.0.0 are larger, and in general it has a sharper gradient within the marginal ice zone (Figure 12). The concentration differences are larger in the summer than in the winter, particularly for the high concentrations within the central pack (cf. Figure 11); therefore, they have a larger effect on the summer time series of area. The larger concentrations within HadISST.2.1.0.0 are due to our choice of reference data set (the post-1994 NIC sea ice charts), relative to which all adjustments and concentration estimations are made.

The time series of the NASA Team sea ice extent and area are given by the blue curves in Figure 10. The extents are lower than in HadISST.2.1.0.0, particularly for July. It should be noted that for the years 1979 to 1996, HadISST1.1 was based on a NASA Team product that was processed at NASA Goddard Space Flight Center, similar to the NSIDC NASA Team product used here. The relatively small differences during this period between these two products are therefore likely due to HadISST1.1 containing monthly medians rather than means. It can be seen that the HadISST.2.1.0.0 extents and areas are larger than those for the NASA Team data. Again, this is due to our choice of reference data set and our attempt to adjust any biases in the passive microwave data due to effects such as thin ice. The relative differences are particularly noticeable in the time series of area for July (dotted curves in Figure 10b), due to melt pond effects in the passive microwave retrievals.

4.1.2. Comparison With DMI Ice Charts

During the years 1901 to 1956 (with a gap during the World War II years, from 1939 to 1945), DMI published an annual report entitled "The State of the Ice in the Arctic Seas". These reports contained monthly charts between April and August (and very occasionally September) that consisted of observations (in red), an estimated ice limit (white), and sometimes a climatology (dashed line), see Figure 13. Information was obtained from Canada, Germany, Great Britain, Norway, Sweden, the U.S., and Russia. The observations came from naval and merchant shipping, shore observers, and in later years from aircraft reconnaissance. The estimated ice edges were based on a mixture of the observations, extrapolation, and climatology. The observational

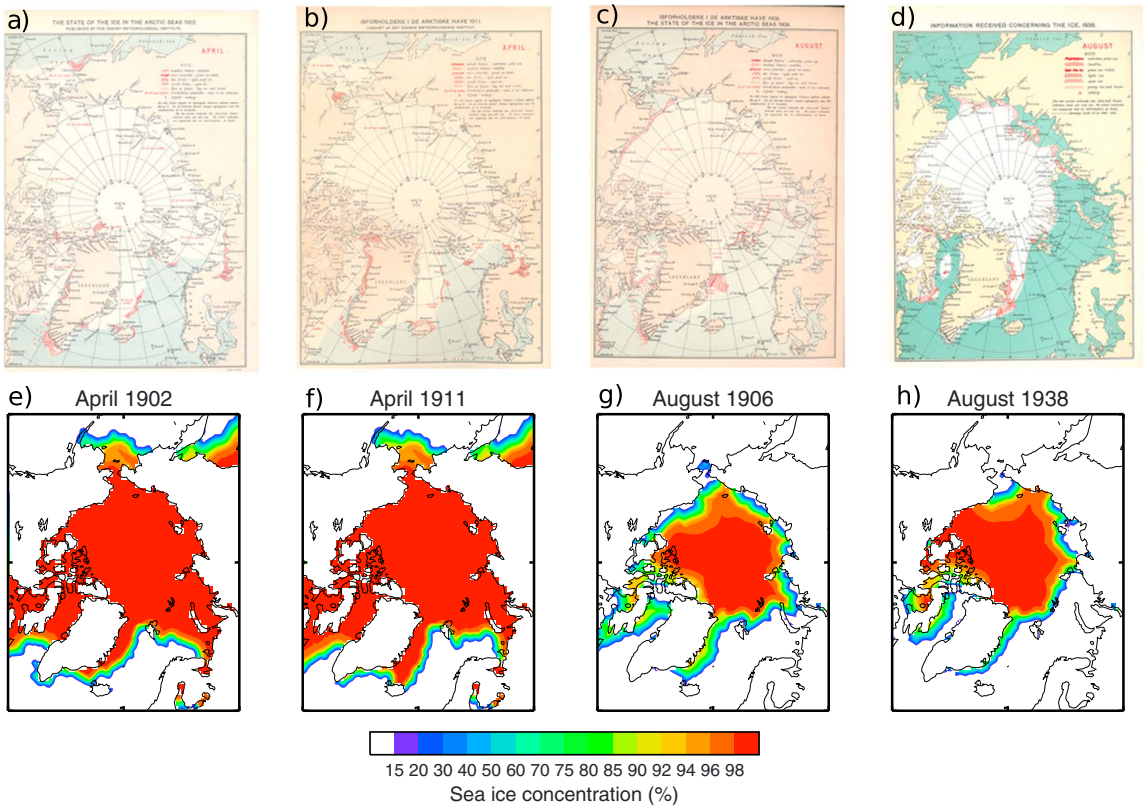

Figure 13. Northern Hemisphere sea ice concentration. (top row) Danish ice charts. (bottom row) HadISST.2.1.0.0. (a and e) April 1902, (b and f) April 1911, (c and g) August 1906, and (d and h) August 1938. On the Danish charts sea ice observations are given in red (with the exception of the red triangles which denote icebergs), the estimated extent of ice is given by the region of white, and the open water is shaded in blue.

coverage was reasonable around Greenland, Iceland, and Spitsbergen. Elsewhere, particularly in the Western Arctic, the observational coverage was poor.

The DMI ice charts were first digitized by *Kelly* [1979] and used in the Walsh and Chapman Arctic compilation (section 2.3). However, they have now been scanned by the Icelandic Meteorological Office and have been made available by NSIDC [*Danish Meteorological Institute and National Snow and Ice Data Center*, 2012] (http://nsidc.org/data/g02203.html). They can provide a useful comparison to HadISST.2.1.0.0 since Walsh and Chapman presented only end of month information and we have attempted to create a monthly analysis here. As only visual comparisons can be made, we are unable to do a thorough assessment through the whole time series. Figure 13 compares some examples of the DMI ice charts (Figures 13a–13d) with the corresponding HadISST.2.1.0.0 concentration fields (Figures 13e–13h). It can be seen that there are regions where the ice edges agree as well as regions where they disagree. In April 1902 (Figures 13a and 13e) there is very good agreement around the Barents Sea, Greenland Sea, the southern tip of Greenland, and the Bering Sea. There is perhaps a little too much ice around Baffin Bay and the Davis Strait in HadISST.2.1.0.0 compared to the ice chart. In April 1911 (Figures 13b and 13f) there is good agreement again, except on the southern tip of Greenland which is missing ice in HadISST.2.1.0.0 compared to the ice chart, and the Davis Strait and the Smith Sound/Nares Strait (in the northern part of Baffin Bay), which contain too much ice. August 1906 (Figures 13c and 13g) shows a fairly extensive year, whereas August 1938 (Figures 13d and 13h) has a lot less ice. In both years HadISST.2.1.0.0 has a small amount of ice around the Bering Strait and the Gulf of Ob (which flows into the Kara Sea), whereas the ice charts are ice-free in these regions. Compared to the ice charts, 1906 also shows a bit too much ice in HadISST.2.1.0.0 in the west of the Chukchi Sea, along the coast, but otherwise shows fairly good agreement. However, in 1938 HadISST.2.1.0.0 contains a lot more ice than the ice charts along the coast of Siberia, particularly in the Laptev Sea and the East Siberian Sea. HadISST.2.1.0.0 therefore does not capture the full severity of the low ice extent that is seen in the ice chart for 1938. These differences between HadISST.2.1.0.0 and the

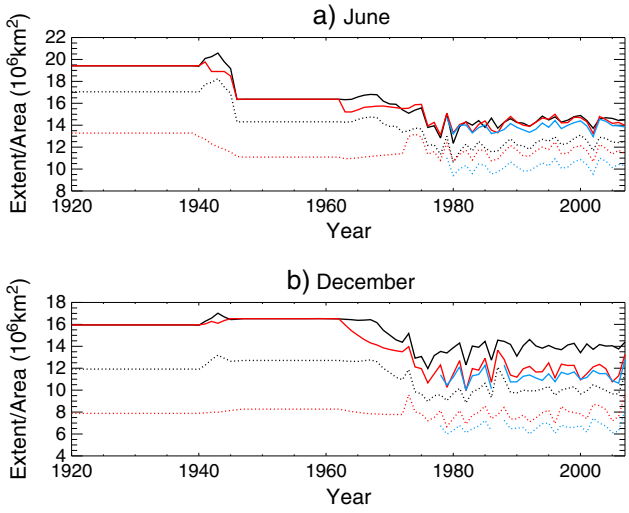

Figure 14. Time series of Southern Hemisphere sea ice extent (solid) and area (dotted), 1920–2007, for HadISST.2.1.0.0 (black), HadISST1.1 (red), and NASA Team (blue). Monthly mean values are shown for (a) June and (b) December.

Danish ice charts may be due either to mistakes made in digitization or in the temporal bias adjustments applied (either by Walsh and Chapman or within the development of HadISST.2.1.0.0). Comparisons with the original Walsh and Chapman data for these months (not shown) show that most of these differences are due to the temporal adjustments applied. In these examples there often appears to be very little adjustment (if any) to the Walsh and Chapman data, which results in too much ice in HadISST.2.1.0.0 following the adjustments from end of month values to monthly mean values. The case where there is less ice in HadISST.2.1.0.0 than in the ice charts (April 1911 at the Southern tip of Greenland) is likely to be due to errors in the Walsh and Chapman data (either during the processing/adjustments or from the digitization).

4.2. Southern Hemisphere

4.2.1. Comparison With HadISST1.1 and NASA Team Passive Microwave Retrievals

In this section we compare HadISST.2.1.0.0 with HadISST1.1 and the NASA Team data as in section 4.1.1. As the South Pole is over land, there are no missing concentrations in the NASA Team data due to a hole at the pole. Figure 14 shows the time series of extents and area for June and December. It can clearly be seen that both HadISST.2.1.0.0 and HadISST1.1 are dominated by climatologies prior to 1973. It should be noted that the years 1850 to 1919 have been excluded from Figure 14 as this period contains the German Atlas climatology (for 1929 to 1939) that continues until 1939 (section 3.5). In June the two time series of extents are very similar after 1972, as is the case throughout most of the calendar year. In December (and November), however, it can be seen that the extents are much larger in HadISST.2.1.0.0 than HadISST1.1 from about 1973 due to the bias adjustments made. As in the NH, the area is larger in HadISST.2.1.0.0 due to the larger concentrations within the ice pack and a shorter marginal ice zone (see Figure 15 for December). This is particularly noticeable in the period prior to 1973 that is based on the two Atlas climatologies (sections 2.4 and 3.5). Despite there being apparently much larger extents throughout this period compared to the later period (Figure 14), the area of ice in HadISST1.1 is relatively small. This is due to the method used to estimate the concentrations within the ice edge in *Rayner et al.* [2003]; the concentrations appear to have been underestimated relative to the passive microwave data used in the development of the method. This resulted in an error in the distribution of concentrations within HadISST1.1 and an incompatibility between the time series of area and extent.

In the period between the two Atlas climatologies as well as the period between the Russian climatology and the NIC charts, it can be seen that the HadISST.2.1.0.0 extents and areas sometimes increase before they decrease. This feature is particularly noticeable in the period 1940–1946 in June, when there is a large difference between the two climatologies. This is an effect of the linear interpolation of the grid box concentrations (section 3.5) and occurs when the ice becomes more extensive in one region and less extensive in another. The ice growth in the interpolated fields occurs at a faster rate than the ice retreat due to the nonlinear distribution of the concentrations within the ice pack in each region of change. It is likely that this effect is larger in

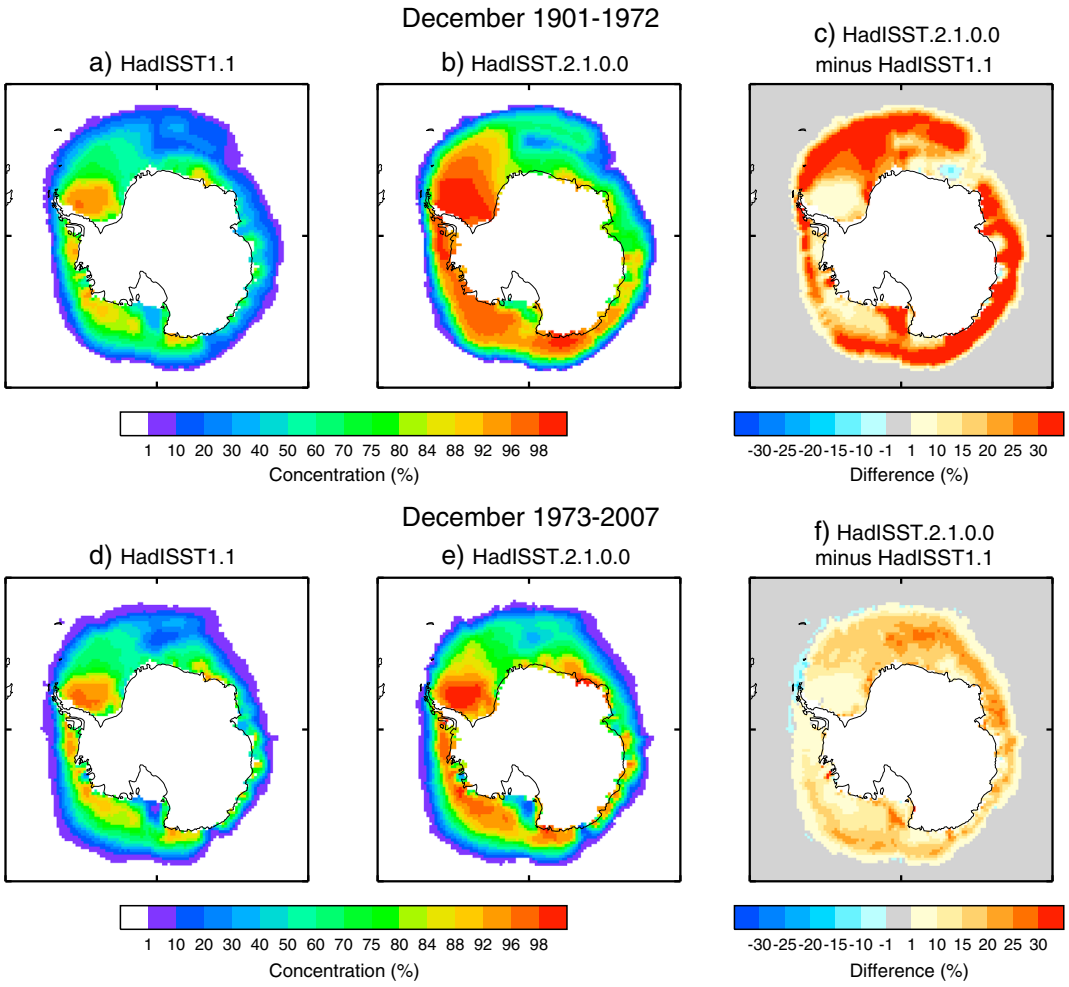

Figure 15. Southern Hemisphere mean sea ice concentration fields and differences in December for (top row) 1901–1972 and (bottom row) 1973–2007. Mean concentrations are given for (a and d) HadISST.2.1.0.0 and (b and e) HadISST1.1. (c and f) Differences in the mean fields.

HadISST.2.1.0.0 due to the shorter marginal ice zone. It can also be seen in the time series of area in HadISST.2.1.0.0 as the concentrations have been reestimated based on the extents, unlike in HadISST1.1.

The time series of NASA Team sea ice extent and area can also be seen in Figure 14 (blue curves). The extents are slightly lower than in both versions of HadISST in June. In December they are much lower than HadISST.2.1.0.0 and a little lower than HadISST1.1. HadISST1.1 Antarctic concentrations and extents were adjusted relative to a passive microwave product [*Hanna and Bamber*, 2001] that was based on the Bristol algorithm [*Smith*, 1996]. This resulted in larger values for the extent and area in the Southern Hemisphere for HadISST1.1. The NASA Team time series of area is relatively low compared to HadISST.2.1.0.0. This is due to our attempt to adjust any biases in the Antarctic passive microwave retrievals caused by thin ice, wet snow, etc., and our choice of reference data set.

4.2.2. Comparison With Southern Ocean Ice Reports

Between the years 1928 and 1954 (except for a gap during the World War II years in 1939–1945) the journal *The Marine Observer* published "Southern Ocean Ice Reports" (hereafter referred to as SOIR, [*The Meteorological Committee, Air Ministry, London*, 1928-1954]). These contained observations of ice from ships around the Antarctic, and although they mainly reported ice bergs, they also contained many references to sea ice (which usually included the type of ice) covering the years 1926 to 1953. The ice observations have now been digitized, and we have compared some of the sea ice positions recorded with the Antarctic Atlas climatologies (sections 2.4 and 3.5). The ice reports appear to be independent of the observations that the Atlas climatologies were based on [*Deutsches Hydrographisches Institute*, 1950; *Tolstikov*, 1966].

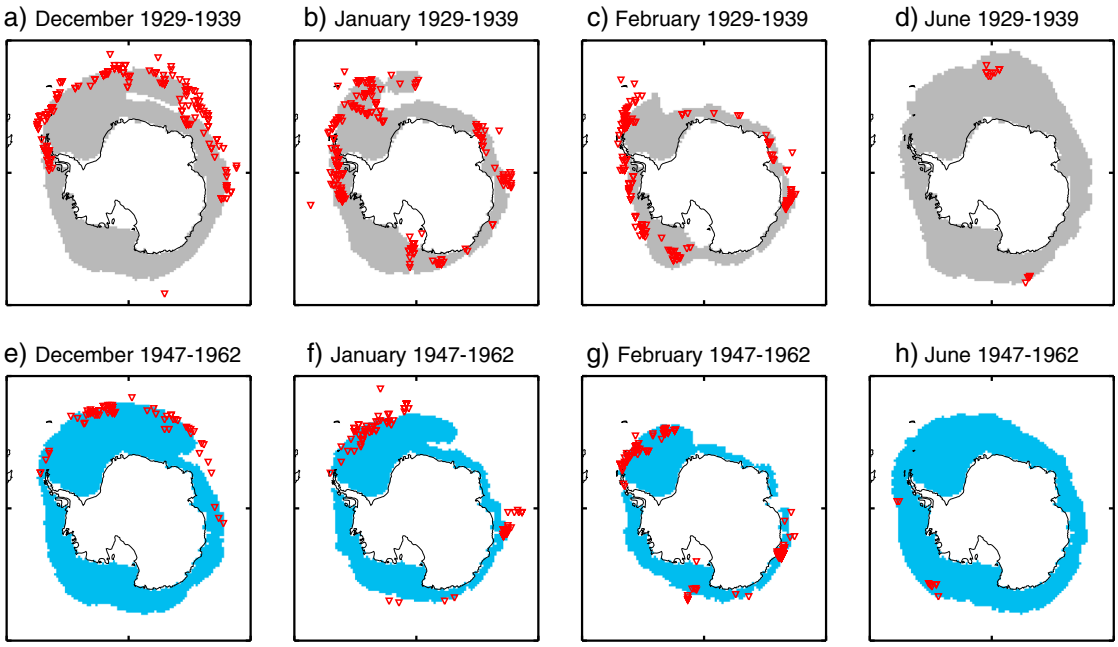

Figure 16. A comparison of sea ice observations digitized from the Southern Ocean Ice Reports (red) with the HadISST.2.1.0.0 climatologies for (top row) 1929–1939 (grey, based on the German Atlas) and (bottom row) 1947–1962 (blue, based on the Russian Atlas). Comparisons for (a and e) December, (b and f) January, (c and g) February, and (d and h) June are shown. Note that there were no observations for the years 1939 and 1954–1962 in the Southern Ocean Ice Reports.

The ice reports mainly contain observations in the summer months, although there are some that are found in the winter months. This is usual for historical sources of sea ice, as conditions are obviously worse in the winter months making it harder for any expeditions. Figure 16 compares the SOIR observations that overlap with the German climatology period (Figures 16a–16d) and the Russian climatology period (Figures 16e–16h) for the months of December, January, February, and June. The SOIR observations sometimes consists of a number of segments that cover several degrees longitude, which indicates that the ship was likely to have skirted along the edge of the main ice pack. The observations agree very well with the two climatologies giving us confidence in the large extents that are seen in HadISST.2.1.0.0 relative to the recent period, which is much better observed (Figure 14). Some small differences between the climatologies and ice reports can be seen. These are expected as the ice reports contain some annual variability, which is not captured by the climatologies.

5. Conclusions and Discussion

In this study we have developed the sea ice concentration component of HadISST.2.1.0.0, the Met Office Hadley Centre monthly sea ice and SST data set, from 1850 to 2007. Primary input data sources include OSI SAF passive microwave data since November 1978 and NIC sea ice chart data prior to this, beginning in 1972 in the Arctic and in 1973 in the Antarctic. Prior to the NIC sea ice charts the Walsh and Chapman compilation was used in the Arctic, and Atlas climatologies were used in the Antarctic. NIC chart data for 1995 to 2007 in the Arctic and 2003 to 2007 in the Antarctic were chosen as our reference data set and assumed to provide the most accurate analysis of the true conditions. Bias adjustments were derived for the OSI SAF data relative to the reference and then propagated back in time using periods of data set overlaps where possible. A new method to estimate concentrations when we only had information about the ice edge was developed using the adjusted passive microwave data. It was then applied to the Walsh and Chapman data and the Atlas climatologies. The data were combined to create global monthly mean analyses on a 1° longitude by 1° latitude grid.

The aim of this work was to create a more consistent global record of sea ice concentrations than HadISST1.1 by using new data sources, applying new bias adjustments, and improving the method used in the estimation of concentrations when only information about the ice edge is known. A comparison of extents and area has shown that HadISST.2.1.0.0 appears to be more homogenous than HadISST1.1. This is in part due to

improved bias adjustments in the later part of the record. In the Arctic, adjustments were large in the summer months as melt ponds on the surface of the ice result in the underestimation of concentrations by passive microwave retrievals. The new adjustments removed a discontinuity seen at the start of the passive microwave record in HadISST1.1, in November 1978. Bias adjustments were also large in the Antarctic summer, where concentrations are also underestimated by the passive microwave retrievals (possibly due to the presence of snow or slush). There is also no longer a discontinuity in 1996/1997 (as was the case in HadISST1.1), as a consistent passive microwave product has been used throughout.

Improved homogeneity is also due to a new and improved method that has been developed to estimate concentrations where only the ice edge is known (as in the Antarctic prior to 1973) or when the fields of Arctic concentration were heterogeneous in time and space prior to 1972 (here concentrations have been reestimated as we prioritized the homogeneity within the data set). In the Antarctic this removed a negative bias seen in the time series of HadISST1.1 area, and in the Arctic this removed discontinuities from the Walsh and Chapman concentration fields in time and space. In both cases this has made the distribution of early concentrations consistent with the later part of the record, based on the bias-adjusted passive microwave retrievals.

Overall, HadISST.2.1.0.0 contains more ice than HadISST1.1 as a result of the reference data chosen (NIC charts for the period 1995 to 2007 in the Arctic and 2003 to 2007 in the Antarctic). This is partly due to larger extents in some calendar months and within some periods but is also the result of an increase in the concentrations within the ice pack and a narrower marginal ice zone.

There is plenty of scope for further improvements to HadISST.2.1.0.0. We envisage releasing further versions as improvements are made. Currently, we have made no improvements to the Great Lakes and Caspian Sea, and the HadISST.2.1.0.0 data in these regions originate from HadISST1.1. Very little sea ice information is available for the Caspian Sea, and so it is unlikely that we would be able to make much progress in this region in the short term, but we would like to reexamine the Great Lakes' concentrations.

NSIDC have traced the ice edge position of the DMI ice charts (on which the Walsh and Chapman data are based prior to 1953) "in order to obtain the ice edge position at a higher resolution than has previously been possible" [*Danish Meteorological Institute and National Snow and Ice Data Center*, 2012] (http://nsidc.org/data/g02203.html). The data will provide a useful addition to our knowledge of Arctic sea ice during this period once they become available and will help with our understanding of the reliability of the Walsh and Chapman data.

NSIDC has also released the data set "Sea Ice Charts of the Russian Arctic in Gridded Format, 1933–2006" [*Arctic and Antarctic Research Institute*, 2007], containing sea ice charts from the Arctic and Antarctic Research Institute (AARI). This is clearly a useful source of information for the Arctic [*Mahoney et al*., 2008], and we feel it would provide a valuable addition to the Walsh and Chapman data prior to the start of the NIC chart data, especially during the winter months and in the years 1939–1952 which are primarily climatology based in Walsh and Chapman. However, the AARI data set only covers the Siberian sector of the Arctic and the region of data is not consistent over time, and so care must be taken so as not to introduce discontinuities when merging the two sources in time and space. Sudden jumps in the position of the ice edge can easily be introduced when this is done, as well as unrealistic changes in time (e.g., features can disappear and reappear in consecutive concentration fields).

We would like to improve the method used to infill the gaps between the climatology periods in the Antarctic. The linear interpolation of the grid box concentrations results in an ice edge that changes more quickly in regions where the ice grows than in regions where it retreats. Ideally, the ice edge would change position at a steady rate in both cases. The HadISST.2.1.0.0 Antarctic time series is clearly still lacking data prior to 1973 and is only based on climatologies before this time. The Southern Ocean Ice Reports data could be incorporated, but there are very few observations and these are not sufficient to incorporate annual variability into the time series in a meaningful way by themselves. We are currently imaging further promising sources of Antarctic sea ice information that could be digitized and used in later versions of HadISST. Research into how ice observations from ships compare to the later NIC ice charts and passive microwave retrievals is also required.

We would also like to make further changes to the method that estimates the concentrations based on the ice edge (section 3.3). At present, land-locked ice is usually set as the high value as it is often some distance

away from any open water. However, in the Arctic summer lower concentrations can sometimes be seen along the coastlines in the passive microwave record; therefore, our method may underestimate the concentrations in these situations. Since completing this work it has come to our attention that there is a small error in our estimation of the concentrations based on the ice edge, which affects the period up until 1971 in the Arctic and 1972 in the Antarctic (i.e., the data based on Walsh and Chapman and the Antarctic atlas climatologies). It only affects a few grid boxes at the very edge of the ice, resulting in slightly less ice than intended and in some cases open water rather than a concentration of 15%. This does not affect the main results within this study and will be corrected for in the next version of HadISST (likely to be version 2.1.1.0).

We have already produced a 0.25° resolution version of HadISST.2.1.0.0 since 1972 in the Arctic and 1973 in the Arctic (section 3.6), and clearly there is potential for a 0.25° resolution daily bias-adjusted passive microwave product from 25 October 1978. The daily fields would require quality control and estimation where gaps exist within the record before any adjustments could be calculated and applied. A daily product could be used to calculate more accurate temporal bias adjustments, which were based here on the unadjusted daily OSI SAF passive microwave data (e.g., for the NIC chart data, section 3.2, and the Walsh and Chapman data, section 3.4).

We have begun work on investigating uncertainties in the sea ice concentrations; however, this is still in the very early stages. Ideally, we would like to produce multiple realizations of the sea ice concentration fields, using the ensemble to explore uncertainties in the data. There are clearly large uncertainties involved, particularly for the historical sources that are based on records of sea ice edges (such as the Walsh and Chapman, section 2.3, and the Antarctic alas climatologies, section 2.4). Uncertainties arise from the accuracy of the observations (they are usually based on point observations), the observational coverage (this is usually very poor), and the estimation of the concentrations (a large scatter can be seen in Figure 7, which indicates large uncertainties in the method used). The latter method also includes the assumption that the ice edge corresponds to the 15% monthly mean concentration contour; this is uncertain and can depend upon the character of the ice (whether it is compact or diffuse). Fields based on climatology have an additional source of uncertainty arising from the large interannual variability of the concentration fields. The later data clearly contain significant uncertainties as well. The OSI SAF uncertainty estimates are given as standard deviations and do not take into account surface effects such as melt ponding. The large scatter seen in Figure 3 indicates that very large differences exist between the NIC charts and the OSI SAF retrievals. This can also be seen in comparisons of their individual monthly fields (not shown). Often the position of the ice edge and the features seen in the concentration fields differ. We also need to investigate how the OSI SAF and NIC chart uncertainties mentioned in sections 2.1 and 2.2 propagate into the monthly mean regridded values calculated within this study. Many of the uncertainty components are large for individual grid box values but are also spatially correlated. An added complication to the calculation of the sea ice uncertainties is that concentration values are bounded by 0 and 1, often skewing the distribution of the uncertainties. All these issues require a better understanding before multiple realizations of the HadISST.2.1.0.0 sea ice fields can be produced. We would also like to strongly encourage other researchers to produce a centennial-scale bias-adjusted sea ice analysis, as this would provide a measure of the structural uncertainty arising from the methodological choices made during the data set construction.

We caution against the use of HadISST.2.1.0.0 for trend analysis in (i) the Arctic prior to 1953, when the fields are often based on climatology (especially during winter months) and (ii) the Antarctic prior to 1973, particularly as the data consist of climatologies that are based on sparse ship observations.

As discussed in section 2.1, OSI SAF plans to release a new product in 2014 that can be used for subsequent updates to their reprocessed concentration data set and therefore HadISST.2.1.0.0. We plan to first use version 1.1 to update HadISST.2.1.0.0 to 2009 and will then use the new product to update our data set to 2013 and provide regular monthly updates after that.

The HadISST data set is freely available to researchers. Version 2.1.0.0 will be released after publication of the three parts of the paper describing it (this study and two papers currently in preparation by Kennedy et al. and Rayner et al.), followed by subsequent versions once they become available. Full documentation will be provided, and the most recent version will be updated monthly. Further information can be found at http://www.metoffice.gov.uk/hadobs/hadisst2/.

Acknowledgments
This work was supported by the Joint DECC/Defra Met Office Hadley Centre Climate Programme (GA01101) and by the EU FP7 ERA-CLIM project. We would like to thank Lynsey McColl for her help with developing the bias adjustment method and Esben Nielsen for converting the Antarctic NIC chart shapefiles to a 25 km EASE grid. We would also like to thank Glyn Hughes for scanning the Southern Ocean Ice Reports and Gail Kelly for digitizing the Southern Ocean Ice Reports. This paper was improved following constructive suggestions from three reviewers.

References

Andersen, S., R. T. Tonboe, S. Kern, and H. Schyberg (2006), Improved retrieval of sea ice total concentration from spaceborne passive microwave observations using Numerical Weather Prediction model fields: An intercomparison of nine algorithms, *Remote Sens. Environ.*, *104*, 374–392.

Andersen, S., R. Tonboe, L. Kaleschke, G. Heygster, and L. T. Pedersen (2007), Intercomparison of passive microwave sea ice concentration retrievals over the high-concentration Arctic sea ice, *J. Geophys. Res.*, *112*, C08004, doi:10.1029/2006JC003543.

Arctic and Antarctic Research Institute (2007), *Sea Ice Charts of the Russian Arctic in Gridded Format, 1933-2006*, edited by V. Smolyanitsky et al., National Snow and Ice Data Center, Boulder, Colo., doi:10.7265/N5D21VHJ.

Cavalieri, D. J., P. Gloersen, and W. J. Campbell (1984), Determination of sea ice parameters with the Nimbus-7 SMMR, *J. Geophys. Res.*, *89*, 5355–5369, doi:10.1029/JD089iD04p05355.

Cavalieri, D., C. Parkinson, P. Gloersen, and H. J. Zwally (1996), *Sea Ice Concentrations From Nimbus-7 SMMR and DMSP SSM/I-SSMIS Passive Microwave Data*, Nov. 1978 to Dec. 2007, National Snow and Ice Data Center, Boulder, Colo. [Updated yearly.]

Cavalieri, D. J., and C. L. Parkinson (2012), Arctic sea ice variability and trends, 1979–2010, *Cryosphere*, *6*, 881–889, doi:10.5194/tc-6-881-2012.

Chapman, W. L., and J. E. Walsh (1991), Long-range prediction of regional sea ice anomalies in the Arctic, *Weather Forecasting*, *6*(2), 271–288.

Comiso, J. C. (1986), Characteristics of arctic winter sea ice from satellite multispectral microwave observations, *J. Geophys. Res.*, *91*, 975–994, doi:10.1029/JC091iC01p00975.

Compo, G. P., et al. (2011), The twentieth century reanalysis project, *Q. J. R. Meteorol. Soc.*, *137*, 1–28, doi:10.1002/qj.776.

Danish Meteorological Institute and National Snow and Ice Data Center (2012), *Arctic Sea Ice Charts From Danish Meteorological Institute, 1893–1956*, Compiled by V. Underhill and F. Fetterer, National Snow and Ice Data Center, Boulder, Colo., doi:10.7265/N56D5QXC.

Dedrick, K., K. Partington, M. Van Woert, C. A. Bertoia, and D. Benner (2001), U. S. National/Naval Ice Center digital sea ice data and climatology, *Can. J. Remote Sens.*, *27*(5), 457–475.

Deutsches Hydrographisches Institute (1950), Atlas of ice conditions in the North Atlantic Ocean and general charts of the ice conditions of the North and South Polar regions, 2335, Hamburg, Germany.

Fetterer, F. (2006), A selection of documentation related to National Ice Center Sea Ice Charts in Digital Format, Special Report 13, National Snow and Ice Data Center, nsidc.org/pubs/documents/special/nsidc_special_report_13.pdf.

European Organisation for the Exploitation of Meteorological Satellites (EUMETSAT) Ocean and Sea Ice Satellite Application Facility (2010), Global sea ice concentration reprocessing dataset 1978–2009 (v1.0), [Online], Norwegian and Danish Meteorological Institutes. [Available at http://osisaf.met.no].

Hanna, E., and J. Bamber (2001), Derivation and optimization of a new Antarctic sea-ice record, *Int. J. Remote Sens.*, *22*(1), 113–139, doi:10.1080/014311601750038884.

Hewitt, H. T., D. Copsey, I. D. Culverwell, C. M. Harris, R. S. R. Hill, A. B. Keen, A. J. McLaren, and E. C. Hunke (2011), Design and implementation of the infrastructure of HadGEM3: The next-generation Met Office climate modelling system, *Geosci. Model Dev.*, *4*, 223–253, doi:10.5194/gmd-4-223-2011.

Inoue, J., J. A. Curry, and J. A. Maslanik (2008), Application of aerosondes to melt-pond observations over Arctic Sea ice, *J. Atmos. Oceanic Technol.*, *25*(2), 327–334, doi:10.1175/2007JTECHA955.1.

Keen, A. B., H. T. Hewitt, and J. K. Ridley (2013), A case study of a modelled episode of low Arctic sea ice, *Clim. Dyn.*, *41*, 1229–1244, doi:10.1007/s00382-013-1679-y.

Kelly, P. M. (1979), An arctic sea ice data set, 1901–1956. Glaciological Data, Report GD-5: Workshop on Snow Cover and Sea Ice Data, World Data Center-A for Glaciology [Snow and Ice], 101–106.

Kusunoki, S., T. Nakaegawa, O. Arakawa, and I. Yagai (2009), Simulations of land-surface air temperature and land precipitation in the twentieth century by the MJ98 AGCM, *J. Meteorol. Soc. Jpn.*, *87*, 473–495, doi:10.2151/jmsj.87.473.

Mahoney, A. R., R. G. Barry, V. Smolyanitsky, and F. Fetterer (2008), Observed sea ice extent in the Russian Arctic, 1933–2006, *J. Geophys. Res.*, *113*, C11005, doi:10.1029/2008JC004830.

McLaren, A. J., et al. (2006), Evaluation of the sea ice simulation in a new coupled atmosphere-ocean climate model (HadGEM1), *J. Geophys. Res.*, *111*, C12014, doi:10.1029/2005JC003033.

Meier, W. N., J. Stroeve, and F. Fetterer (2007), Whither Arctic sea ice? A clear signal of decline regionally, seasonally, and extending beyond the satellite record, *Ann. Glaciol.*, *46*, 428–434, doi:10.3189/172756407782871170.

Meier, W. N., J. Stroeve, A. Barrett, and F. Fetterer (2012), A simple approach to providing a more consistent Arctic sea ice extent time series from the 1950s to present, *The Cryosphere*, *6*, 1359–1368, doi:10.5194/tc-6-1359-2012.

National Ice Center (2006), *National Ice Center Arctic Sea Ice Charts and Climatologies in Gridded Format*, 1972 to 2007, Compiled by F. Fetterer and C. Fowler, National Snow and Ice Data Center, Boulder, Colo., doi:10.7265/N5X34VDB.

National Ice Center, Fleet Numerical Meteorology and Oceanography Detachment, and National Climatic Data Center (1996), *Arctic and Antarctic Sea Ice Data 1972–1994*, CD-ROM Version 1.0.

Notz, D., and J. Marotzke (2012), Observations reveal external driver for Arctic sea-ice retreat, *Geophys. Res. Lett.*, *39*, L08502, doi:10.1029/2012GL051094.

Parker, D. E., M. Jackon, and E. B. Horton (1995), The GISST2.2 sea surface temperature and sea ice climatology, *Clim. Res. Tech. Note CRTN 63*, Met Office Hadley Centre, Bracknell, U. K.

Parkinson, C. L., J. C. Comiso, and H. Zwally (2004), *Nimbus-5 ESMR Polar Gridded Sea Ice Concentrations*, edited by W. Meier and J. Stroeve, NASA DAAC at the National Snow and Ice Data Center, Boulder, Colo.

Partington, K., T. Flynn, D. Lamb, C. Bertoia, and K. Dedrick (2003), Late twentieth century Northern Hemisphere sea-ice record from U.S. National Ice Center ice charts, *J. Geophys. Res.*, *108*(C11), 3343, doi:10.1029/2002JC001623.

Rayner, N. A., E. B. Horton, D. E. Parker, C. K. Folland, and R. B. Hackett (1996), Version 2.2 of the global sea ice and sea surface temperature data set, 1903 – 1994, *Clim. Res. Tech. Note CRTN74*, Hadley Cent., Met Office, Bracknell, U. K.

Rayner, N. A., D. E. Parker, E. B. Horton, C. K. Folland, L. V. Alexander, D. P. Rowell, E. C. Kent, and A. Kaplan (2003), Global analyses of sea surface temperature, sea ice, and night marine air temperature since the late nineteenth century, *J. Geophys. Res.*, *108*(D14), 4407, doi:10.1029/2002JD002670.

Scaife, A. A., et al. (2009), The CLIVAR C20C project: Selected 20th century climate events, *Clim. Dyn.*, *33*, 603–614, doi:10.1007/s00382-008-0451-1.

Shokr, M., and L. Kaleschke (2012), Impact of surface conditions on thin sea ice concentration estimate from passive microwave observations, *Remote Sens. Environ.*, *121*, 36–50, doi:10.1016/j.rse.2012.01.005.

Smith, D. M. (1996), Extraction of winter total sea ice concentration in the Greenland and Barents Seas from SSM/I data, *Int. J. Remote Sens.*, *17*, 2625–2646.

Stroeve, J., M. M. Holland, W. Meier, T. Scambos, and M. Serreze (2007), Arctic sea ice decline: Faster than forecast, *Geophys. Res. Lett.*, *34*, L09501, doi:10.1029/2007GL029703.

Stroeve, J. C., M. C. Serreze, M. M. Holland, J. E. Kay, J. Maslanik, and A. P. Barrett (2011), The Arctic's rapidly shrinking sea ice cover: A research synthesis, *Clim. Change*, doi:10.1007/s10584-011-0101-1.

Stroeve, J. C., V. Kattsov, A. Barrett, M. Serreze, T. Pavlova, M. Holland, and W. N. Meier (2012), Trends in Arctic sea ice extent from CMIP5, CMIP3 and observations, *Geophys. Res. Lett.*, *39*, L16502, doi:10.1029/2012GL052676.

The HadGEM2 Development Team (2011), The HadGEM2 family of Met Office Unified Model climate configurations, *Geosci. Model Dev.*, *4*, 723–757, doi:10.5194/gmd-4-723-2011.

The Joint WMO-IOC Technical Commission for Oceanography and Marine Meteorology (2008), Proceedings of the Ice Analysts Workshop, Rostock, Germany, 12–17 June 2008, WMO/TD-No. 1441. [Available at ftp://ftp.wmo.int/Documents/PublicWeb/amp/mmop/documents/JCOMM-TR/J-TR-43-IAW-2008/index.htm.]

The Meteorological Committee, Air Ministry, London (1928–1953), Southern Ocean Ice Reports, The Marine Observer, 5-24.

Tolstikov, E. I. (1966), *Atlas of the Antarctic*, vol. 1, 126 pp., Glav. Uprav. Geod. Kart, MGSSSR, Moscow.

Uppala, S. M., et al. (2005), The ERA-40 re-analysis, *Q. J. R. Meteorol. Soc.*, *131*, 2961–3012, doi:10.1256/qj.04.176.

Walsh, J. E. (1978), A data set on Northern Hemisphere sea ice extent. World Data Center-A for Glaciology (Snow and Ice), *Glaciological Data, Report GD-2*, part 1, pp. 49–51.

Walsh, J. E., and W. L. Chapman (2001), Twentieth-century sea ice variations from observational data, *Ann. Glaciol.*, *33*, 444–448.

Walsh, J. E., and C. M. Johnson (1978), Analysis of Arctic sea ice fluctuations 1953-77, *J. Phys. Oceanogr.*, *9*(3), 580–591.